International Journal Of
Industrial Electronics Control and Optimization
Print ISSN: 3517-2645
Online ISSN: 3568-2645
Homepage: https://ieco.usb.ac.ir/

The Stochastic P2P Energy Management Scheme for Integrated Energy Microgrid Considering P2G and Electricity Network Fee

Meysam Feili[1] | Mohammad Taghi Ameli[2*]

Department of Electrical Engineering, University of Shahid Beheshti, Tehran, Iran [1,2]
Corresponding author's email: m_ameli@sbu.ac.ir

Article Info

Article type:
Research Article

Article history:
Received: 13-June-2024
Received in revised form: 18-August-2024
Accepted: 20-August-2024
Published online: 21-March-2025

Keywords:
Integrated energy systems,
Microgrids,
Stochastic optimization,
AC power flow,
Peer-to-peer energy market.

ABSTRACT

The prominent role of natural gas networks in mitigating the intermittency of renewable energy resources has highlighted the importance of integrated operation between electricity and gas grids. Additionally, energy storage systems, such as batteries and hydrogen, play a crucial role in power balancing and energy management. Previous research on the synergy between electricity and natural gas systems has primarily focused on the operational constraints of each grid. Only a few studies have explored market-driven models, such as peer-to-peer (P2P) energy trading, for the integrated operation of these networks. Furthermore, the limited studies that have implemented the peer-to-peer (P2P) market model for the integrated operation of power and natural gas grids have been conducted in two distinct phases: scheduling and trading. This paper introduces a stochastic P2P market-based optimization model for the coupled operation of natural gas and electricity grids, considering smart grid technologies such as power-to-gas (P2G) storage, batteries, and demand response (DR). Also, the presented framework incorporates alternating current (AC) power flow, natural gas steady-state model, and the power grid usage fee through the electrical distance model. The simulation results indicate that the proposed method significantly decreases total operating costs, reduces power losses, improves network component synergy, and enhances the performance of both networks.

	Indices	S^{fit}	Feed − in tariff price ($/kWh)
i, j	Index of network's node	S^{gas}	Natural gas tariff ($/kWh)
s	Index of scenarios	P^{dem}	Power demand (MW.)
n	Index of reduced scenarios	$\phi^{flex,MAX}$	Max demand flexibility(%)
t	Index of time (hour)	$\phi^{flex,MIN}$	Min demand flexibility(%)
N_{ng}	Nanogrid node	η_{dec}	The efficiency of battery discharging (%)
N_{gt}	Gas turbine node	η_{ch}	The efficiency of battery charging (%)
N_e	Power grid node	SOC(0)	Initial SOC level of battery (MWh)
N_g	Natural gas node	SOC^{min}	Min SOC level
N_{p2g}	P2G node	SOC^{max}	Max SOC level
N_{gc}	Gas compressor node	$PR.^{min}$	Gas pressure minimum level (psi)
	Constants	$PR.^{max}$	Gas pressure maximum level (psi)
S^{rit}	Electricity price ($/kWh)	G	The real part of the admittance matrix
S^{cur}	Power shedding penalty ($/kWh)	B	The imaginary part of the admittance matrix
$\mathbb{C}\phi_{ch}^{p2g}$	The conversion coefficient of P2Gs (MW/kg)	$P^{grid,ramp}$	Tie line power ramp rate (MW/h)
$E^{init,p2g}$	Initial stored hydrogen in the container (kg)	D	Diameter of the pipeline (m)
η_{p2g}^{ch}	The P2G charging efficiency	S	The cross − section area of the pipeline (m^2)
η_{p2g}^{dch}	The P2G discharging efficiency		
$P^{Min,Max,gt}$	Min and Max constraint of gas turbine (MW.)		
$P^{gt,ramp}$	Ramp rate limit of gas turbines (MW/h)	$P^{dch,m}$	Discharging power inside a Nanogrid (MW)
V^{min}	Lower bound of node voltage (kV)	SOC^{batt}	Battery SOC level

Copyright © Mohammad Taghi Ameli (s).
Publisher: University of Sistan and Baluchestan

V^{max}	Upper bound of node voltage (kV)	g^{gt}	Gas turbine′s natural gas burn rate (m^2)
Δh	Height disparity between nodes (m)	$q^{Gen,gt}$	Gas turbine′reactive power output (MVAr)
$d_{i,j}$	The sum of the electrical distances	G^{line}	Natural gas flow rate (m^2)
$Z_{i,j}$	Thevenin impedance distance	Pr^{grid}	Node gas pressure (psi)
$u_{i,j}^{dis}$	Distance unit fee($/per_distance_unit)	e	Node voltage′s real component
a, b, c	constants of the gas turbine′s heat rate funct	f	Node voltage′s imaginary component
λ	Friction coefficient of the Darcy factor	$q^{Dem,MG.}$	Total injected reactive power (MVAr)
Z	The factor of gas compressibility	S^{grid}	apparent power (MVA)
R	Constant of natural gas (J/(kg K))	$P^{p2g,Dch}$	The P2G discharged power (MW)
L	Gas pipeline length (m)	$P^{p2g,ch}$	The P2G charged power (MW)
Temp	Gas flow average temperature (K)	$E^{tot,p2g}$	the total hydrogen in the container (kg)
β_{comp}	Coefficient of gas compressor	$E^{dch,p2g}$	The discharged hydrogen (kg)
η_{comp}	Efficiency of gas compressor	$E^{ch,p2g}$	The charged hydrogen (kg)
$G^{comp,max}$	Maximum permissible gas flow through the compressor (m^2)	$P^{Dem,N}$	Nanogrid demand supplied by the power grid (MW)
$P^{comp,max}$	Maximum allowable gas compressor power demand (MW)	$P^{NG,GT}$	Nanogrids traded energy with gas turbines (MWh)
	Abbreviation	$P^{NG,P2G}$	Nanogrids traded energy with P2Gs (MWh)
P2P	Peer to peer	$P^{P2G,N}$	P2G energy purchased from the power grid (MWh)
DERs	Distributed energy resources	$P^{P2G,GT}$	P2G energy purchased from the gas turbine (MWh)
DR	Demand response	$P^{P2G,NG}$	P2G energy sold to the Nanogrids (MWh)
CDA	Continuous double auction	$P^{N,P2G}$	P2G energy sold to the power grid (MWh)
DSO	Distribution system opera	$P^{GT,P2G}$	Gas turbine energy sold to the P2G (MWh)
MINLP	Mixed integer none leaner programming	$P^{GT,NG}$	Gas turbine energy sold to the Nanogrid (MWh)
FIT	Feed − in tariff rate	S^{P2P}	Final P2P Price ($/MW)
ESS	Energy storage system	$P^{Gen,N}$	Gas turbine generated power to the grid (MW)
TID	$Thevenin\ impedance\ distance$	$P_{i,t}^{comp}$	Gas compressor power demand (MW)
	Decision Variables	$G_{i,t}^{comp}$	Compressor gas flow rate m^2
$q^{dch,n}$	Discharging ESS reactive power to grid (MVAr)	DV	Binary decision variable
$Q^{Dem,N}$	Reactive power supplied by the power grid (MVAr)	G^{grid}	Injected natural gas into the gas grid's nodes (m^2)
$P^{Dem,NG}$	Active power supplied by the power grid (MW)	$Pr_{i,t}^{out}$	Outlet pressure of gas compressor (psi)
P^{cur}	Curtailed power (MW)	$Pr_{i,t}^{in}$	Inlet pressure of gas compressor (psi)
$q^{Dem,DR.}$	Reactive power demand after scheduling (MVAr)	$q_{i,t}^{p2g,dch}$	The P2G discharged reactive power (MVAr)
G^{grid}	Injected natural gas (m^2)	$q_{i,t}^{p2g,ch}$	The P2G charging reactive power (MVAr)
$P^{Gen,gt}$	Gas turbine active power output (MW)	$q_{i,t}^{comp}$	Gas compressor reactive demand (MVAr)
$P^{Dem,DR.}$	The power demand of Nanogrid (MW)	φ^{dis}	network charge $/per distance unit
P^{ch}	ESS′s charging power (MW)	q^{cur}	curtailed reactive power (MVAr)
$P^{Tot,dch}$	Total discharging power (MW)	ψ	traded energy ($/kWh)

I. Introduction

In traditional power systems, electricity flows in a single direction. In such systems, large, centralized power plants generate electricity, and the generated power is transmitted through the grid to consumers [1]. However, due to increasing electricity demand, environmental concerns, and declining fossil fuel reserves, policymakers are advocating a shift from centralized to distributed power systems [2-5] .Recent studies suggest integrating Distributed Energy Resources (DERs) can result in cleaner and more reliable energy systems with substantial environmental benefits [6-8]. Nonetheless, the increasing integration of DERs at the consumer premises transforms power system control, presenting new operational challenges [9, 10].

A microgrid (MG) is a part of the power distribution grid that can be controlled and coordinated, either connected to the main grid or islanded operation [11, 12]. MGs can lower transmission line losses and enhance power quality [13]. They utilize various DERs such as solar panels, wind turbines, micro-hydro systems, and gas turbines as power sources, thereby addressing energy shortages and enhancing grid efficiency [14-18]. The advancement of DER technologies has emphasized energy management within MGs. To mitigate

power fluctuations from renewable DERs, gas turbines with flexible features are increasingly deployed on the demand side to smooth out renewables' intermittent nature. Employing gas turbines to address balancing issues highlights the significance of integrating the operation of electricity and natural gas systems [19].

Local energy trading through the Peer-to-peer (P2P) market is an innovative technology that enables customers to purchase and sell electricity within a local energy market. This P2P market framework provides significant flexibility, enhanced control over energy usage, and lower customer bills. It also allows for more efficient utilization of DERs [20, 21]. The emergence of the energy-sharing market is supported by advancements in information and communication technologies, alongside the deregulation of power distribution grids, which together facilitate P2P energy trading among local energy resources. Research in this area spans multiple domains, including communication infrastructure, market design, policy-making, social science, and trading platforms [22].

The advent of Power-to-Gas (P2G) technology heralds a transformative approach to energy conversion and storage, offering a promising avenue for mitigating renewable energy intermittency and decarbonizing the energy sector. P2G entails the conversion of surplus-generated electricity into hydrogen gaseous fuels through electrolysis and subsequent chemical processes [23]. This innovative technology holds immense potential in addressing the challenges posed by the variable nature of renewable energy sources or market price volatility by storing excess energy in the form of easily transportable and storable gases [23]. Moreover, P2G systems offer versatility by integrating renewable energy into existing gas infrastructure, facilitating its utilization across various sectors, including transportation, industry, and heating.

Battery storage systems represent a pivotal advancement in energy storage, offering scalable and flexible solutions to intermittency and grid stability associated with renewable energy integration [24]. Battery systems utilize electrochemical processes to store surplus electricity, thereby enabling its utilization during periods of high demand or when renewable generation is insufficient [25]. Battery storage enhances grid reliability and resilience while optimizing renewable energy utilization by mitigating curtailment and enabling smoother integration into existing grids [25]. Furthermore, advancements in battery technology, coupled with declining costs, have rendered battery storage an economically viable option for both grid-scale and distributed applications, thereby catalyzing its widespread adoption and deployment [26]. Demand response (DR) mechanisms represent a critical component of modern energy management strategies, offering a means to balance supply and demand in real-time by adjusting electricity consumption patterns in response to grid conditions or price signals. DR initiatives empower consumers to actively participate in grid operations by voluntarily reducing or shifting their electricity usage during peak periods or in response to fluctuating energy prices [27].

Gas-fired generators, renowned for their flexibility, are considered valuable resources for integrating renewable-based distributed energy resources (DERs) into the power grid, thereby linking the power and natural gas systems. This interdependence highlights the importance of coordinating natural gas and electricity networks. Meanwhile, P2P energy market technology is an emerging solution that enables local energy trading among customers, aiding the integration of diverse DERs into the power system. By employing the P2P energy trading model to coupled natural gas and electricity systems, substantial benefits can be realized for all market participants. Many researchers have considered the integrated operation of electricity and natural gas grids.

Wang et al. [28] present a P2P energy trading market designed explicitly for the microgrids (MGs) community, taking into account the operating costs of the power grid during the market-clearing process. Zhang et al. [1] proposed bi-level multi-energy trading (hydrogen and electricity) in the integrated energy systems considering day ahead and real-time balancing markets. It did not consider the electricity and natural gas grid constraints, renewable energy resources, P2Gs, and load flexibility. Crespo-Vazquez et al. [29] offer a framework for P2P energy trading that maintains user preferences and encompasses both day-ahead and intraday markets. They introduce a two-stage stochastic programming model for managing the day-ahead market: in the first stage, users decide the amount of energy they are willing to trade in real-time, and in the second stage, battery operations (charging and discharging) are determined. Authors of [30] proposed the integrated operation of natural gas and electricity grids, facilitating synergy between gas turbines, electricity consumers, and P2Gs. It did not consider both grid constraints. Optimal pricing and market equilibrium are addressed by [31] to create a P2P trading strategy between community MGs and the energy balance service provider. The presented case studies show significant economic benefits for the service provider. Reference [32] developed a novel transactive energy management system framework that integrates P2P and peer-to-grid energy trading through efficient and fair energy pricing strategies. The authors tried to create a peer-to-grid market instead of the FIT rate to facilitate energy trading between prosumers and the power grid. This paper focuses on the energy markets and does not consider the operation of natural gas and electricity networks.

Authors of [33] employed the multi-objective game-theoretic optimization method to facilitate P2P energy trading and applied the Nash equilibrium game to determine the optimal number of participants and payoffs for P2P and peer-to-grid energy trading. Rowe et al. [34] proposed bi-level optimization for an electrical-heat-hydrogen-gas multi-energy

storage system. In the upper level, an MILP was implemented to reduce investment and operation costs. Additionally, the model incorporates grid support criteria at the lower level to reduce network losses. The reviewed paper did not consider batteries, DR, and the gas compressor's role in the integrated energy systems model. The study in [35] introduced a P2P energy trading model that employs neural networks to lower operational costs and implement peak shaving. Despite its notable contributions, the approach lacks integration of trading mechanisms and power network models within the proposed P2P market framework.

Authors in [36] proposed a decomposed P2P energy trading method considering the effect of transacted energy on the power network stability and minimized information exchange between agents and between agents and the grid operator. This paper focused on developing a decentralized framework for P2P energy trading. It did not consider the integrated operation of gas and power networks, ESSs, DR, and P2G.

The authors of [37] explored prosumers' social cooperation through a coalition formation game for the P2P energy market. Reference [38] addressed integrating electricity and natural gas markets by using gas turbines and P2G systems as connecting points between the gas and power grids and examined various clearing strategies to maximize customer profits. Niu et al. [39] proposed a P2P energy trading model in which electricity consumers traded with the electricity producer (transmission system operator) and the natural gas wholesale market (gas supplier). This paper focuses on designing a novel P2P market that allows consumers to trade gas directly from different natural gas suppliers. It did not consider P2G, DR, and the effect of energy transactions on both grids' performance.

Authors of [40] developed an integrated market for power and heat energies, considering electric heating appliances as energy coupling points. This study examined the clearing prices in various energy markets and evaluated how energy consumption patterns influence market competition by employing the AC power flow method.

Reference [41] proposed a method for coupling heating, power, and natural gas energies via a P2P market. However, this paper did not assess the effectiveness of the proposed framework on the functionality of the natural gas and electricity grids. Researchers in [42] designed a P2P energy trading mechanism for prosumers using a coalition graph game, enabling them to form coalitions and determine the quantity and price of traded energy. In this study, the Myerson value rule is used to fairly distribute the total payoff of the P2P scheme among customers. Numerical analysis shows prosumers can benefit from the P2P scheme while adhering to local voltage constraints. Lu et al. [43] present a framework where the power generated by producers is first transmitted to the distribution network, and then purchasers receive the same amount of power minus the distribution network's power losses. Reference [44] proposed a P2P market for sharing a DR between customers. In the first stage, the entity named IEO centrally runs an optimization problem to determine the customer energy schedule for the day ahead market. Due to customers' arbitrary behaviors or renewable power fluctuations, a decentralized P2P market was performed in the second stage to exchange the DR between customers. Also, the reviewed paper did not consider the effect of DR sharing on the performance of the gas and power systems.

Basnet and Zhong [45] suggest a one-hour ahead market where a market operator clears the energy equilibrium price and schedules DERs. In this setup, the transmission network acts as a generator when supplying energy to a community and as a consumer when the community sells its surplus energy. Wang et al. [46] developed a game-theory-based P2P market that allows customers to trade both heat and electricity, considering cooperative behavior among trading agents. This market design explores the synergistic utility of multi-energy trading within an integrated energy system. Zhou et al. [47] propose a two-level congestion management model to meet security constraints. Although their framework provides financial benefits to end customers through participation in the local flexibility market, it does not establish a new framework for this market. Reference [48] integrates various types of energy systems using a two-phase mixed integer linear programming algorithm and hybrid power flow calculation to determine market clearing prices for power, natural gas, and heat energies. Wang et al. [49] propose an innovative risk-averse market-clearing method for integrated power, district heating, and natural gas systems, employing a stochastic framework to mitigate financial risks associated with the intermittency of wind power generation. They use a locational marginal price model to incentivize market participants. Hutty et al. [50] proposed a P2P energy trading framework based on the continuous double auction (CDA) method to trade electricity and heat. This paper considered a CDA-based P2P market to create a local energy market that enabled customers to exchange electricity and heat energies. It did not consider the gas and power networks, DR, and uncertainties.

Zhang et al. [51] proposed a P2P energy trading market for commercial buildings, focusing on multi-energy coupling to enhance energy efficiency and reduce operating costs. However, this study does not address grid constraints and energy transaction fees. Chen et al. [52] introduced a two-level bidding strategy to optimize energy trading within household neighborhoods, taking into account energy storage systems (ESS) and photovoltaic generation. Despite its novel approach, this paper does not consider the impact of energy trading on power grid performance. Jiang et al. [53] proposed a two-stage optimization framework to maximize customer benefits in P2P energy trading. The first stage determines the amount of energy bought or sold in the market. The second stage organizes the market and facilitates energy trading

among customers. However, the paper has some limitations: the two separate stages are not optimal, and the framework's impact on the performance of both networks is not considered.

As shown in Table 1, While we have reviewed many existing works, most reviewed papers conducted in the P2P energy trading frameworks do not consider the coupled operation of electricity and natural gas systems via the P2P energy trading market. Additionally, the few papers that have considered the P2P market framework for the integrated operation of natural gas and electricity networks have explored various methods for designing a decentralized energy trading framework. On the other hand, methods like P2P energy trading are tools that incentivize customers to generate and consume power locally, considering both grids' and customers' benefits. Hence, considering the effects of energy transactions on the performance of gas and power distribution grids is crucial.

Integrating the detailed AC power flow method and natural gas model to evaluate the effect of the P2P energy transaction on the performance of both grids is a vital research aspect not considered in the previous papers. Also, proposing the P2P framework in which the customers' energy schedules are determined based on the market price rather than the power utility price is another research gap that needs to be addressed. Also, considering different energy storage systems such as P2Gs and batteries and using their potential advantages in the P2P market is another research gap. Reference [54] proposed the model and framework for the P2P market based on the CDA method, which was performed in two separate stages. Also, the authors of [4] borrowed the P2P energy market model from the reference [54] and proposed a two-stage framework to integrate the operation of gas and electricity grids through the P2P market framework, considering both network models and constraints. Employing a two-stage framework for P2P energy trading is not optimal, but it is applicable [54]. There are two reasons why this strategy is not optimal for all market players. First, a subscriber's payment cost is determined by the prices specified in the P2P energy trading agreements, not by the electricity prices offered by the power utility used in the objective function. Additionally, the customers choose the amount of electricity to sell or purchase and the bid or ask price in two separate stages instead of jointly at one step [54]. Therefore, a P2P energy trading scheme needs to be developed to schedule DERs based on the P2P market clearing price and consider the effect of each energy transaction on the performance of both grids.

Incentivized by the research gap in the literature, in the first step, we developed a novel joint P2P optimization mechanism for the integrated operation of electricity and natural gas systems considering the AC power flow framework and natural gas steady-state model. The word “joint” implies that the customers' energy is scheduled by the objective function based on the P2P market price. Also, employing both network models (the AC power flow and natural gas steady-state model) enables the network operators to precisely track the energy transaction's effect on the electricity (the voltage profile) and natural gas (node gas pressure) grids. To consider the power grid fee during energy trading and reduce the electricity network losses, we borrowed the Thevenin impedance distance (TID) model from previous literature and engaged it with the optimization problem. Using the TID model enables the network operator to consider the effect of line losses on each energy peer. To harness the different energy storage flexibility through the P2P local energy market, we consider the P2G units and battery storage in the proposed model.

TABLE 1 OVERVIEW OF THE LITERATURE REVIEW

Ref.	Year	IO	P2P	IONPS	AC Power flow	PNUF	DR	P2G
[50]	2024	×	✓	✓	×	×	×	✓
[47]	2022	×	✓	×	✓	×	✓	×
[55]	2021	×	✓	×	×	×	×	×
[1]	2024	✓	✓	×	✓	×	×	×
[56]	2024	×	✓	✓	×	×	×	×
[1]	2024	×	✓	×	×	×	×	×
[57]	2021	×	×	✓	✓	×	✓	×
[22]	2022	×	✓	×	×	×	×	×
[58]	2022	×	✓	×	×	×	×	×
[59]	2022	×	✓	×	✓	×	✓	×
[60]	2022	×	✓	×	✓	×	✓	×
[61]	2022	×	✓	×	×	×	×	×
[62]	2021	×	✓	✓	×	✓	×	×
[53]	2022	×	✓	×	×	×	×	×
[51]	2022	×	✓	✓	×	×	×	×
[22]	2023	×	✓	×	×	×	×	×
[4]	2023	✓	✓	✓	✓	×	×	×
This paper		✓	✓	✓	✓	✓	✓	✓

** Integrated optimization (IO)
Integrated operation of natural gas and power systems (IONPS)
Power network usage fee (PNUF)

In the following, to show the proposed method's superiority and examine its strengths and drawbacks, we compared the presented framework with the benchmark method based on the continuous double auction CDA mechanism, executed in two separate stages [54]. In summary and order of priority, the novelties of this paper are as follows:

- This paper proposes a novel stochastic P2P-based optimization problem for integrated energy microgrid scheduling to facilitate synergy between different DERs (P2Gs, nano grids (NGs), ESSs, and gas turbines) regarding both network constraints.
- Proposing a scenario-based stochastic model for considering natural gas and electricity demands uncertainties to give a better perspective for network operators.
- Considering the electricity network’s usage price based on the electrical distance model, the AC power flow model, the DR, different energy storage

technology (P2G and ESS), and the natural gas steady-state model.

The remainder of this paper is organized as follows: Section 2 introduces the relevant ideas of the presented P2P market design for the incorporated operation of natural gas and electricity networks. Section 3 describes the P2P-based optimization problem (mathematical model) driven by the electric distance between purchasers and vendors. In Section 4, numerical studies are introduced to show the advantages of the presented method. The conclusion and proposed future research aspects are presented in section 5.

II. Methodological framework

This paper introduces the novel electrical distance-based approach for the incorporated operation of natural gas and electricity systems via the P2P market framework at the microgrid level. The proposed microgrid is equipped with a distribution system operator (DSO). Also, we suppose that the DSO is responsible for operating the electricity and natural gas networks [10, 63]. In this regard, the primary target of this paper is to design a joint P2P energy trading-based market for the incorporated operation of electricity and natural gas networks to facilitate the synergy between customers such as consumers (NGs), prosumers (ESSs and P2Gs), and producers (gas turbines). The proposed method is in such a way that the amount of energy to be sold/ purchased in the market is determined based on the market pieces rather than the power utility prices, considering the effect of electrical distance on the transaction fees, the AC power flow, the steady state natural gas grid model and the electricity demand flexibility.

The centralized P2P markets have the advantage of maximizing the welfare of the entire community. Another benefit of centralized P2P frameworks is that the power generation and consumption patterns of peers are more predictable, which reduces uncertainty. The reason is that the coordinator, the DSO, directly controls the operational status of peers [64]. The computational complexity and users' privacy autonomy issues are considered significant drawbacks of centralized methods [64]. Considering that the development of decentralized energy trading is not within the scope of this paper, we employed a simple centralized framework. In this regard, the DSO centrally solves the proposed P2P optimization problem. How to propose the decentralized framework in the joint P2P energy market for the incorporated operation of natural gas and electricity grids remains to be studied, but it is not the focus of this paper. Fig. 1. Illustrates the proposed method's timeline.

As evident from Fig.1, the presented method consists of three major parts. In the first section, the DSO gathers information related to the network components, such as the electricity network and natural gas grid data, customers' related settings, etc. Then, in the second stage, the DSO executes the joint P2P energy trading-based optimization problem to determine the trading schedule for the next 24 hours. In this regard, the targeted period of the optimization problem is the day-ahead market. The presented framework is implemented on the integrated energy microgrid that comprises a 33-bus power distribution grid and a modified 33-node natural gas network. The natural gas and electricity grids are integrated through gas compressors and gas-fired generators. The presented competitive local market price enables customers such as P2Gs to participate in the local energy market, which increases the total social welfare.

The architecture of the proposed method is presented in Fig. 2. The structure of the presented microgrid consists of four main components, including gas turbines (producer), NGs (prosumer), P2Gs (prosumer), the distribution power network (lines and transformers), and natural gas distribution network (lines and compressors). All microgrid components send the required information and settings to the DSO. After gathering information, the DSO solves the P2P-based optimization problem to determine the customer's trading schedules considering the electrical distance between customers, the DR, and both grid constraints. The output of the optimization problem is customers' energy trading schedules, consisting of energy trading plans with other customers or the power grid. The DSO is responsible for balancing bids and offers that are not matched during the P2P market procedure. In this regard, customers' shortage/surplus energy, which is not matched in the P2P energy trading market, is supplied/purchased by the power grid. Employing the AC power flow method and natural gas steady-state model enables the DSO to monitor the detailed effect of energy transactions on the performance of electricity and natural gas grids. The presented P2P-based optimization problem is in such a way that energy transactions between customers reduce the power losses, maintain the node gas pressure in the allowable interval, reduce the total operating expenses of the microgrid, and increase the profit of gas turbines and P2Gs.

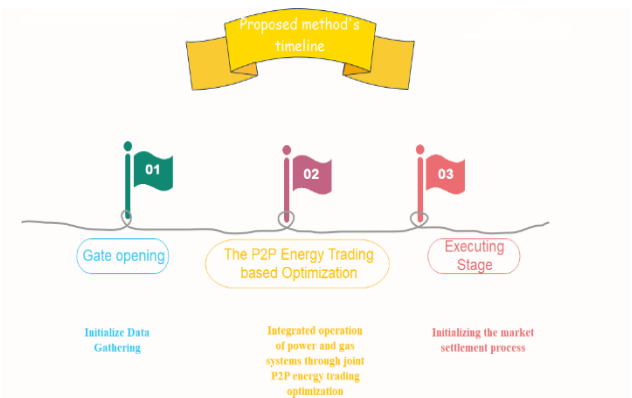


Fig. 1. The presented method timeline.

III. P2P-based optimization problem

As mentioned, this paper considers an integrated energy microgrid consisting of NGs, P2G units, gas turbines, and

ESSs. NGs have power and natural gas demands; natural gas is used for heating and cooking. Also, no control action is placed on the gas loads in NGs. Three types of electrical loads (fixed, emergency, and flexible) are considered at the NGs level. As the name suggests, the fixed loads are noncontrollable and nonadjustable. Emergency loads refer to those groups of power demand that can not be adjusted or curtailed. The difference between fixed and emergency loads is that fixed loads can be curtailed, but emergency loads cannot be interrupted. Flexible loads refer to those groups of electrical loads that can control and adjust their demand profiles across different timescales. Thermostatic loads, ESS, and electric vehicle fleets are examples of flexible loads. The electricity and natural gas load profiles for the next 24 hours are available to the NG operator. Also, NGs are equipped with an ESS, and it is assumed that NGs do not have renewable energy sources. The MG's decision variables are the optimal power demand of NGs (supplied by the power grid and the P2P energy market), ESSs' charging/discharging cycle, optimal charging/discharging cycles of P2Gs (purchased/sold from/to the power grid or the P2P market), and energy generation schedules of gas-fired generators (sold to the electricity grid or local consumers via the P2P energy market).

This paper uses the gas turbine unit as a fossil fuel-based power generation system. The inherent flexibility of gas turbines, characterized by their rapid ramping rate and quick response time, renders them particularly well-suited to managing the intermittency inherent in modern power systems [65]. The DSO gathers various information from the MG's different components. The NGs predicted electricity and natural gas demands for the next 24 hours, P2Gs-related data, gas turbines' rated capacity, the power grid's various data, and related information of the natural gas pipeline are part of the collected information by the DSO. After decision-making and processing, the optimization results are transmitted to the customers as energy trading schedules. The energy trading schedules include energy trading plans between customers and the power grid.

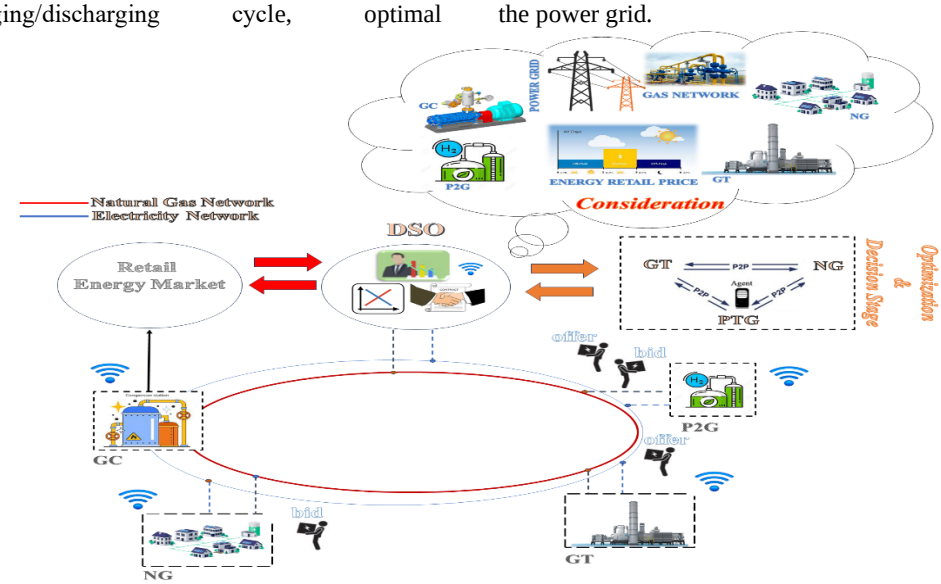


Fig. 2. The overall framework of the proposed method.

The presented framework is based on the mixed integer nonlinear problem (MINLP) optimization programming, which the DSO centrally solves to obtain customers' optimal P2P energy trading schedule. The MINLP is a mathematical optimization approach that involves solving problems with both continuous and discrete (integer) variables where the objective function or some of the constraints are nonlinear. The objective function of the P2P-based optimization problem, shown in Equation (1), is based on the day-ahead market structure.

In the objective function, the first three terms are costs related to energy purchased by the NGs. The second four terms are costs and revenues related to the P2G units. After the P2Gs' related terms, the following terms are the penalty related to the curtailed energy of NGs, the revenue related to selling stored energy to the power grid, and the cost of supplying natural gas from the wholesale natural gas price. The last four terms are revenues related to gas turbines' traded energy and gas compressor operation costs. The gas compressor's electricity demand is supplied only by the power grid through the energy retail price.

For the sake of simplicity, we suppose that the energy stored in the ESSs' is consumed within the NGs or sold to the power grid. The power utility, P2G units, and gas turbines supply the NGs' power demands. Also, the power generated by gas turbines is purchased by the power grid, P2Gs, and NGs. In this regard, the power grid balances surplus production and consumption.

As it is clear from Equation (1), The total operating cost of the microgrid is related to the market price (S^{P2P}), the FIT rate (S^{fit}), the natural gas wholesale price (S^{gas}), and retail energy

price (S^{rit}). The FIT rate and retail price are constant, while the market price is determined in the process of P2P-based optimization. The presented objective function reduces NGs' total payment cost and increases gas turbines' and P2Gs' total revenue. Equation (2) shows that the total power demand of NGs ($P_{s,i,t}^{Dem,NG}$) is supplied by the power grid ($P_{s,i,t}^{Dem,N}$) and the P2P energy trading with gas turbines ($P_{s,i,j,t}^{NG,GT}$) and P2Gs ($P_{s,i,j,t}^{NG,P2G}$). The power grid supplies the NGs' power demand, which is not matched in the P2P market.

$$\min\left\{\sum_{s=1}^{n}\Phi_s\left(\sum_{i}^{N_{ng}}\sum_{t}^{T}P_{s,i,t}^{Dem,N}S_{s,i,t}^{rit}\right.\right. \quad (1)$$
$$+\sum_{i}^{N_{ng}}\sum_{j}^{N_{gt}}\sum_{t}^{T}P_{s,i,j,t}^{NG,GT}S_{s,i,j,t}^{P2P}$$
$$+\sum_{i}^{N_{ng}}\sum_{j}^{N_{p2g}}\sum_{t}^{T}P_{s,i,j,t}^{NG,P2G}S_{s,i,j,t}^{P2P}$$
$$+\sum_{i}^{N_{p2g}}\sum_{j}^{N_{gt}}\sum_{t}^{T}P_{s,i,j,t}^{P2G,GT}S_{s,i,j,t}^{P2P}$$
$$+\sum_{i}^{N_{p2g}}\sum_{t}^{T}P_{s,i,t}^{P2G,N}S_{s,i,t}^{rit}$$
$$-\sum_{i}^{N_{p2g}}\sum_{j}^{N_{ng}}\sum_{t}^{T}P_{s,i,j,t}^{P2G,NG}S_{s,i,j,t}^{P2P}$$
$$-\sum_{i}^{N_{p2g}}\sum_{t}^{T}P_{s,i,t}^{N,P2G}S^{fit}$$
$$+\sum_{i}^{N_{ng}}\sum_{t}^{T}P_{s,i,t}^{cur}S^{cur}$$
$$-\sum_{i}^{N_{ng}}\sum_{t}^{T}P_{s,i,t}^{dch,m}S^{fit}$$
$$+\sum_{i}^{N_{g}}\sum_{t}^{T}G_{s,i,t}^{grid}S^{gas}$$
$$-\sum_{i}^{N_{gt}}\sum_{t}^{T}P_{s,i,t}^{Gen,N}S^{fit}$$
$$-\sum_{i}^{N_{gt}}\sum_{j}^{N_{mg}}\sum_{t}^{T}P_{s,i,j,t}^{GT,NG}S_{s,i,j,t}^{P2P}$$
$$-\sum_{i}^{N_{gt}}\sum_{j}^{N_{p2g}}\sum_{t}^{T}P_{s,i,j,t}^{GT,P2G}S_{s,i,j,t}^{P2P}$$
$$\left.\left.+\sum_{i}^{N_{gc}}P_{s,i,t}^{comp}S_{i,t}^{rit}\right)\right\}$$

$$P_{s,i,t}^{Dem,NG}=P_{s,i,t}^{Dem,N}+\sum_{j}^{N_{gt}}P_{s,i,j,t}^{NG,GT}+\sum_{j}^{N_{p2g}}P_{s,i,j,t}^{NG,P2G}\ \forall\ i\in N_{ng},s\in n,t\in T \quad (2)$$

Equations (3) to (5) determine NGs traded energy (with gas-fired generators and P2G units) and P2Gs purchased energy from gas turbines via the P2P market. Also, to determine purchasers and sellers in P2P energy trading, we employed the binary decision variable ($Dv_{s,i,j,t}$), which is shown in Equation (3) to (5). This binary variable makes the model MINLP. The seller and purchaser at time t are determined through the binary decision variable. For instance, in Equation (3), ($Dv_{s,i,j,t}$) Indicates that the NG (i) at the time period (t) purchases ($P_{s,i,j,t}^{NG,GT}$) kWh from the gas turbine (j). In other words, if ($Dv_{1,1,25,10}$) equals 1, which means that in scenario one, NG "1" trades energy with gas turbine "25" at period 10. Also, the amount of energy that gas turbine "25" sells to NG "1" is determined by solving the optimization problem.

$$P_{s,i,j,t}^{NG,GT}=Dv_{s,i,j,t}P_{s,i,j,t}^{GT,NG}\ \forall\ i\in N_{ng},j\in N_{gt},s\in n,t\in T \quad (3)$$

$$P_{s,i,j,t}^{NG,P2G}=Dv_{s,i,j,t}P_{s,i,j,t}^{P2G,NG}\ \forall\ i\in N_{ng},j\in N_{p2g},s\in n,t\in T \quad (4)$$

$$P_{s,i,j,t}^{P2G,GT}=Dv_{s,i,j,t}P_{s,i,j,t}^{P2G,GT}\ \forall\ i\in N_{p2g},j\in N_{gt},s\in n,t\in T \quad (5)$$

As seen in Constraint (6), the total NGs' power demand ($i\in N_{ng}$) supplied from the gas turbine j via the P2P market at the period *t* must be less than or equal to the energy that gas turbine j is considered to share with NGs ($P_{s,i,j,t}^{GT,NG}$). In other words, gas turbines can not sell energy beyond their generated power at period t. Similar constraints (Inequalities (7) and (8)) are considered for traded power between P2Gs and gas turbines and between NGs and P2Gs.

$$\sum_{i}^{N_{ng}}Dv_{s,i,j,t}P_{s,i,j,t}^{GT,NG}\le P_{s,i,j,t}^{GT,NG}\ \forall\ j\in N_{gt},s\in n,t\in T \quad (6)$$

$$\sum_{i}^{N_{p2g}}Dv_{s,i,j,t}P_{s,i,j,t}^{GT,P2G}\le P_{s,i,j,t}^{GT,P2G}\ \forall\ j\in N_{gt},s\in n,t\in T \quad (7)$$

$$\sum_{i}^{N_{ng}}Dv_{s,i,j,t}P_{s,i,j,t}^{P2G,NG}\le P_{s,i,j,t}^{P2G,NG}\ \forall\ j\in N_{p2g},s\in n,t\in T \quad (8)$$

In the P2P-based optimization problem, we suppose the DSO accesses the whole power distribution grid topology. In this regard, the DSO charges the customers for each energy trading based on the power grid's infrastructure usage. The matched price related to trading energy between customers (i) and (j) is shown in Equation (9). The money paid/received by the purchaser/seller for the power grid usage fee is shown in the second term of Equation (9). The network charges are exogenous costs. In this regard, when the customer (i) is a purchaser, its (φ) is positive, which results in total prices higher than trading prices. When the customer (i) is a seller, its receive price is lower than the traded price since parameter φ is negative.

$$S_{s,i,j,t}^{P2P}=\psi_{s,i,j,t}P_{s,i,j,t}^{*,*}\pm\phi_{s,i,j,t}^{dis}P_{s,i,j,t}^{*,*}\quad\forall\ i,j\in N_{*},\ s\in n,t\in T \quad (9)$$

The initial term in Equation (9) corresponds to the price determined by the P2P agreement. The subsequent term represents the grid fee paid to the DSO as a grid operation charge [62]. Beyond operational expenses, these incomes can also be allocated for maintenance, compensation for power losses, and investment expenditures. The Unique Cost Allocation Policy is a common approach for charging customers [66]. This policy distributes costs uniformly among community members, ensuring that grid usage fees are applied without discrimination. However, due to its general application, customers in congested areas may not be incentivized to engage in responsible behavior. Consequently, the misconduct of a few customers can negatively impact the entire customer.

In order to allocate costs more precisely, network charges can be proportional to the electric distance between customers. The TID and power transfer distance are two methods for determining the electrical distance between power network buses. The TID is more suitable for radial networks, while the second is more reliable for mesh networks [66]. This study calculates the electrical distance based on the TID, as formerly presented in [66, 67]. The TID between customer (i) and (j) is presented by Equation (10).

$$Z_{i,j} = \left|\mathcal{R}_{i,i} + \mathcal{R}_{j,j} - \mathcal{R}_{i,j} - \mathcal{R}_{j,i}\right| \quad (10)$$

Where the elements of the TID ($\mathbb{R}$) are the components of the impedance matrix (Z_{Bus}), which is the converse of the admittance matrix (Y_{Bus}). As a result of this cost allocation policy, customers will be encouraged to trade with their closest electrical partners. Due to electricity losses, long electric distance trade is more expensive. When network charge is equally shared between both sides of the trade, it becomes [67]:

$$\phi_{i,j}^{dis} = \frac{u^{dis} d_{i,j}}{2} \quad (11)$$

The ($d_{i,j}$) is the sum of the electrical distances between customers (i) and (j). The parameter (u^{dis}), distance unit fee, is presented in ($/per distance unit). As stated before, we considered the TID method to determine the electrical distance between traders. Fig.3 shows a simple radial network to clarify how the DSO considers the electrical distance between customers in the presented P2P-based optimization. The DSO calculates the network charge based on the electric distance ($Z_{i,j}^{th}$) between nodes using Equation (11).

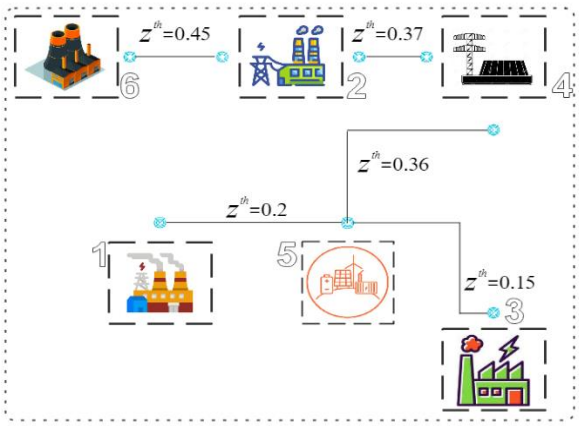


Fig. 3. The sample radial power grid.

The only consumer is placed in node "5" at the simple grid. This customer can trade energy with five producers placed in other nodes with different electric distances. With the assumption that the distance unit fee (u^{dis}) is .01 ($/Km); Table 2 shows the network fee for the illustrative grid in Fig. 3.

TABLE 2 THE SAMPLE RADIAL NETWORK FEE.

node	1	2	3	4	6
$d_{i,j}$	0.2	0.73	0.15	0.36	1.18
$\varphi_{i,j}^{dis}$	$0.001P_{i,j}^{P2P}$	$0.00365P_{i,j}^{P2P}$	$0.00075P_{i,j}^{P2P}$	$0.0018P_{i,j}^{P2P}$	$0.0059P_{i,j}^{P2P}$

As it is clear from Table 2, the network charges gain with increasing the electric distance between purchasers and sellers. So if consumer "5" trades energy with producer "6", its charge is eight times more than trading with producer "3". The market price ($\Psi_{s,i,j,t}$) is bounded by Constraint (12) [46]. This Equation dictates that no consumers are willing to purchase energy above the retail energy price, and no producers are eager to sell energy lower than the FIT rate [46].

$$S^{fit} \le \psi_{s,i,j,t} \le S_t^{rit} \quad \forall\ i,j \in N_*\ s \in n,t \in T \quad (12)$$

We have considered the DR capability in the P2P-based optimization problem to increase customers' profit. In this paper, the load flexibility model is based on [65]. Constraint (13) states that in the period (t) the demand of the NG (i) can be increased by a factor of ($f_{i,t}^{flex,MAX}$). Also, in the following Equations ($P_{s,i,t}^{dem}$) is the NGs predicted load, which is a parameter.

$$P_{s,i,t}^{Dem,DR} \le P_{s,i,t}^{dem} f_{i,t}^{flex,MAX} \quad \forall\ i \in N_{ng}, s \in n, t \in T \quad (13)$$

Similarly, inequality (14) indicates that in the period t, the electrical demand of NGs can be decreased by a factor ($f_{i,t}^{flex,min}$). Equation (15) guarantees that the total energy demand of the NGs (i) does not change after DR. The values

of ($f_{i,t}^{flex,MAX}$) and ($f_{i,t}^{flex,min}$) are determined by the NGs' operator [65].

$$P_{s,i,t}^{Dem,DR} \geq P_{s,i,t}^{dem} f_{i,t}^{flex,MIN} \quad \forall\ i \in N_{ng}, s \in n, t \in T \tag{14}$$

$$\sum_{t}^{T} P_{s,i,t}^{Dem,DR} = \sum_{t}^{T} P_{s,i,t}^{dem} \quad \forall\ i \in N_{ng}, s \in n \tag{15}$$

It is worth noting that we consider the electrical loads with flexible characteristics through simple Equations (13)-(15). Also, in an emergency, the DSO can curtail part of the demand by paying its cost, which is considered in the objective function. Each NG's power balance equation can be found in Equation (16) [4]. The energy demand in NG (i) shall be equal to the imported energy supplied by the power grid, P2G units, and gas turbines represented in Equation (2). The power demand in the NG is divided into two main sections: the power consumed inside NGs ($P_{s,i,t}^{Dem,DR}$) and served to charge the NG's ESS ($P_{s,i,t}^{ch}$).

$$P_{s,i,t}^{Dem,NG} + \left(\eta_{dch} P_{s,i,t}^{dch,n}\right) + P_{s,i,t}^{cur} - \left(\frac{1}{\eta_{ch}} P_{s,i,t}^{ch}\right) - P_{s,i,t}^{Dem,DR} \quad \forall i \in N_{ng}, s \in n, t \in T \tag{16}$$

The mathematical formulas of the NG's ESS are presented in Equations (17)-(18) and Constraint (19) [4]. As it is clear from Equation (17), the stored energy in the ESS can be discharged in the NG ($P_{s,i,t}^{dec,n}$) or sold to the power grid ($P_{s,i,t}^{dec,m}$). As stated before, it is assumed that the energy stored in the ESS can be sold to a power utility or consumed inside the NG.

$$P_{s,i,t}^{Tot,dch} = P_{s,i,t}^{dch,n} + P_{s,i,t}^{dch,m} \quad \forall i \in N_{ng}, s \in n, t \in T \tag{17}$$

Equation (18) calculates each ESS's state of charge (SOC). In order to increase the life span of batteries, their SOC level must remain at a predetermined level, as presented in Constraint (19) [10]. Equation (20) indicates that ESSs are not charged and discharged simultaneously and illustrates charging/discharging limitation [10].

$$SOC_{s,i,t}^{batt} = SOC_{s,i}(0) + \sum_{t=1}^{T} \left(P_{s,i,t}^{ch} - P_{s,i,t}^{Tot,dch}\right) \quad \forall i \in N_{ng}, s \in n \tag{18}$$

$$SOC_{s,i}^{min} \leq SOC_{s,i,t}^{batt} \leq SOC_{s,i}^{max} \ \forall i \in N_{ng}, s \in n, t \in T \tag{19}$$

$$P_{s,i,t}^{ch} \times P_{s,i,t}^{Tot,dch} = 0 \quad \forall\ i \in N_{ng}, s \in n, t \in T$$
$$P_{s,i,t}^{ch} \& P_{s,i,t}^{Tot,dch} \leq P_{ESS}^{max} \quad \forall\ i \in N_{ng}, s \in n, t \in T \tag{20}$$

This paper considers the steady-state natural gas flow model on the day-ahead scheduling time scale. In other words, we assumed that the response time of the natural gas network equals the power grid. According to [68, 69], we can formulate the natural gas network as follows: Injected gas into each grid node is formulated by Equation (21). Gas turbines and NGs are the consumers of the injected natural gas into each node [4, 10].

$$G_{s,i,t}^{grid} = g_{s,i,t}^{gt} + g_{s,i,t}^{load} \quad \forall i \in N_g, s \in n, t \in T \tag{21}$$

As it is clear from Equation (22), the gas turbine's power generation ($P_{s,i,t}^{Gen,gt}$) is sold in the P2P market ($P_{s,i,t}^{GT,NG}$) and ($P_{s,i,t}^{GT,P2G}$) or purchased by the power utility ($P_{s,i,t}^{Gen,N}$).

$$P_{s,i,t}^{Gen,gt} = P_{s,i,t}^{Gen,N} + P_{s,i,t}^{GT,NG} + P_{s,i,t}^{GT,P2G} \ \forall i \in N_{gt}, s \in n, t \in T \tag{22}$$

The performance of thermal plants based on natural gas, coal, and oil fuels is simulated well through quadratic and cubic cost functions [70]. The gas-fired generator natural gas demand is formulated by the quadratic cost function shown in Equation (23) [71]. The fuel cost function coefficients are shown by parameters (a), (b), and (c). The efficiency and construction year of gas turbines determine these coefficients.

$$g_{s,i,t}^{gt} = \alpha_i P_{s,i,t}^{Gen,gt^2} + \beta_i P_{s,i,t}^{Gen,gt} + c_i \forall i \in N_{gt}, s \in n, t \in T \tag{23}$$

The nodal gas flow balance is calculated using Equation (24), which illustrates that injected natural gas equals withdrawn gas. The sum of natural gas injected on gas nodes passes through pipelines. Also, the gas flow is unilateral from the beginning of the gas grid [4].

$$G_{s,i,j,t}^{line} - \sum_{j}^{N_g} G_{s,j,t}^{grid} = 0 \ \ \forall i, j \in N_g, s \in n, t \in T \ \ and\ i < j$$
$$G_{s,i,j,t}^{line} + G_{s,j,i,t}^{line} = 0 \tag{24}$$

Since the proposed natural gas grid's diameter is relatively large, we employed the Weymouth function, shown in Equation (25) [29]. This function shows the relationship between node gas pressure and gas flow in the natural gas pipeline. The TEMP represents the average temperature coefficient of a gas flow, which is considered constant. For more information about the parameter of the Weymouth function, refer to the [29].

$$G_{s,i,j,t}^{line} = \frac{1}{4} \frac{\left|Pr_{s,i,t}^{2}(1 - c\Delta h) - Pr_{s,j,t}^{2}\right| D_{i,j,t} S_{i,t}}{\left(1 - \frac{c\Delta h}{2}\right) \lambda ZRL_{i,j} Temp} \ \forall i, j \in N_g, s \in n, t \in T \tag{25}$$

Natural gas grid node pressure must remain within predetermined ranges to ensure gas supply security, and pressure drops compromise this security. Hence, the natural gas grid node pressure is limited by Constraint (26). The power demand of the gas compressor, which depends on the gas flow rate, is illustrated by Equation (27) [4]. The natural gas rate and power demand constraints of gas compressors are presented consecutively by inequalities (28)-(29) [4].

$$Pr^{min} \leq Pr_{s,i,t} \leq Pr^{max} \ \forall i \in N_g, s \in n, t \in T \tag{26}$$

$$P_{s,i,t}^{comp} = \frac{\beta_{comp} G_{s,i,t}^{comp}}{\eta_{comp}} \left[\left(\frac{Pr_{s,i,t}^{out}}{Pr_{s,i,t}^{in}}\right)^{\frac{1}{\beta_{comp}}} - 1\right] \forall i \in N_{gc}, s \in n, t \in T \tag{27}$$

$$G_{s,i,t}^{comp} \leq G^{comp,max} \ \forall\ i \in N_{gc}, s \in n, t \in T \tag{28}$$

$$P_{s,i,t}^{comp} \leq P^{comp,max} \ \forall\ i \in N_{gc}, s \in n, t \in T \tag{29}$$

Electricity is converted into gaseous fuel through P2G technology. The electrolysis process transforms electricity into hydrogen and oxygen. The generation of hydrogen through the

electrolysis process is demonstrated by Equation (30) [72]. Additionally, Equation (31) details the process of discharging P2G units. The total quantity of hydrogen within the container, measured in kilograms, is determined by Equation (32) [72].

$$E_{s,i,t}^{ch,p2g} = P_{s,i,t}^{p2g,ch} \times \mathbb{C}\!\!\!\!\mathbb{f}_{ch}^{p2g} \forall\, i \in N_{p2g}, s \in n, t \in T \quad (30)$$

$$E_{s,i,t}^{dch,p2g} = P_{s,i,t}^{p2g,dch} \times \mathbb{C}\!\!\!\!\mathbb{f}_{dch}^{p2g} \forall\, i \in N_{p2g}, s \in n, t \in T \quad (31)$$

$$E_{s,i,t}^{tot,p2g} = E_{s,i,t}^{init,p2g} + E_{s,i,t}^{ch,p2g} - E_{s,i,t}^{dch,p2g} \;\forall\, i \in N_{p2g}, s \in n, t \in T \quad (32)$$

Equation (33) indicates that the P2P market and the power grid supply the required power for charging P2Gs. Also, Equation (34) represents that the stored energy in the hydrogen containers can be bought by NGs through the local energy market or the power grid. P2Gs are not allowed to be charged and discharged simultaneously, as represented by Equation (35) [72]. Equation (36) bounds the charging and discharging power of P2Gs [72].

$$\frac{1}{\eta_{p2g}^{ch}} P_{s,i,t}^{p2g,ch} = \sum_{j}^{N_{gt}} P_{s,i,j,t}^{P2G,GT} + P_{s,i,t}^{P2G,N} \;\forall\, i \in N_{p2g}, s \in n, t \in T \quad (33)$$

$$\eta_{p2g}^{dch} P_{s,i,t}^{p2g,dch} = \sum_{j}^{N_{ng}} P_{s,i,j,t}^{P2G,NG} + P_{s,i,t}^{N,P2G} \forall\, i \in N_{p2g}, s \in n, t \in T \quad (34)$$

$$P_{s,i,t}^{p2g,ch} \times P_{s,i,t}^{p2g,dch} = 0 \;\; \forall\, i \in N_{p2g}, s \in n, t \in T \quad (35)$$

$$P_{s,i,t}^{p2g,ch} \& P_{s,i,t}^{p2g,dch} \le P_{p2g}^{max} \quad (36)$$

Equations (37)-(43) illustrate the constraints of the power grid with multiple gas turbines and NGs. Each NG's power demand and gas turbine's generated power regulation affect power flow and the power grid node's voltage [73]. Equations (37) and (38) represent the power flow balance equations for active and reactive powers in the power distribution grid [74].

$$\begin{aligned} P_{s,i,t}^{Dem,MG} + P_{s,i,t}^{Gen,gt} + P_{s,i,t}^{dec,n} + P_{s,i,t}^{cur} & - P_{s,i,t}^{dem,DR} + P_{s,i,t}^{p2g,dch} - P_{s,i,t}^{p2g,ch} - P_{s,i,t}^{comp} \\ &= e_{s,i,t} \sum_{j}^{N_e} \left(G_{i,j} e_{s,j,t} - B_{i,j} f_{s,j,t}\right) \\ &+ f_{s,i,t} \sum_{j}^{N_e} \left(G_{i,j} e_{s,j,t} + B_{i,j} f_{s,j,t}\right) \;\forall i \in N_e, s \in n, t \in T \end{aligned} \quad (37)$$

$$\begin{aligned} q_{s,i,t}^{Dem,MG} + q_{s,i,t}^{Gen,gt} + q_{s,i,t}^{dec,n} + q_{s,i,t}^{cur} & - q_{s,i,t}^{dem,DR} + q_{s,i,t}^{p2g,dch} - q_{s,.i,t}^{p2g,ch} - q_{s,i,t}^{comp} \\ &= f_{s,i,t} \sum_{j}^{N_e} \left(G_{i,j} e_{s,j,t} - B_{i,j} f_{s,j,t}\right) \\ &- e_{s,i,t} \sum_{j}^{N_e} \left(G_{i,j} e_{s,j,t} + B_{i,j} f_{s,j,t}\right) \;\forall i \in N_e, s \in n, t \in T \end{aligned} \quad (38)$$

As shown in Equations (37) and (38), the power injections at the nodes are quadratic functions of the nodes' voltages' rectangular coordination [75]. The ramp rate of tie-line power measures how quickly a power system can adjust its power output in response to changes in demand, which is the essential metric for ensuring the stability of a power system [74]. Constraint (39) formulates the tie line power ramp rate based on (MW/h) [74].

$$\left|P_{s,i,t}^{Dem,N} - P_{s,i,t-1}^{Dem,N}\right| \le P_i^{grid,ramp} \forall i \in N_e, s \in n, t \in T \quad (39)$$

In order to ensure that the voltage magnitude at each node in the power system remains within an acceptable range, Constraint (40) is employed, which is essential to guarantee reliable power system operation and avoid costly equipment damage [74].

$$\left(V_i^{min}\right)^2 \le e_{s,i,t}^2 + f_{s,i,t}^2 \le (V_i^{max})^2 \forall i \in N_e, s \in n, t \in T \quad (40)$$

Apparent power constraint refers to the limitations of a power system caused by factors such as insufficient capacity, network congestion, or high demand. It can create problems such as power outages, reliability issues, and higher costs. Constraint (41) represents apparent power constraints related to each node [74].

$$\left(P_{s,i,t}^{Dem,N}\right)^2 + \left(Q_{s,i,t}^{Dem,N}\right)^2 \le \left(S_{s,i,t}^{Dem,N}\right)^2 \forall i \in N_e, s \in n, t \in T \quad (41)$$

Constraints (42) and (43) demonstrate the gas turbine's output and ramping rate constraints; these constraints are essential for maintaining the gas turbine's efficiency and avoiding damage to the machinery [74].

$$P_i^{Min,gt} \le P_{s,i,t}^{Gen,gt} \le P_i^{Max,gt} \;\forall i \in N_{gt}, s \in n, t \in T \quad (42)$$

$$\left|P_{s,i,t}^{Gen,gt} - P_{s,i,t-1}^{Gen,gt}\right| \le P_i^{gt,ramp} \;\forall i \in N_{gt}, s \in n, t \in T \quad (43)$$

IV. Simiulation and results

A. Assumption

A modified 33-bus natural gas grid and the IEEE 33-node power distribution network are employed to evaluate the presented framework [4]. Characteristics of the natural gas network are chosen from [76]. The number of the electricity network and gas grid nodes is equal [4, 10]. Also, it is assumed that node 0 is the slack bus in the electricity distribution network. The studied microgrid has three types of customers: NGs, P2Gs, and gas-fired generators [4]. In the examined network, it is supposed that all nodes of the natural gas grid have the same altitude. Also, the natural gas grid beside the gas turbines supplies the fixed gas loads in the NGs. The required data for simulation is presented in Table 3.

Fig. 5 represents the time of use of the electricity tariff. The predicted electricity and natural gas demands are borrowed from [4, 77]. The power and natural gas loads are aggregated demands randomly shared between NGs. The calorific value of natural gas is employed to convert gas loads to (MW). Also, it is assumed that each NG is equipped with an ESS.

TABLE 3 REQUIRED PARAMETERS FOR SIMULATION.

Parameter	Value	Parameter	Value
u^{dis}	0.1 ($/km)	SOC_i^{max}, SOC_i^{min}	90%, 20%
Pr^{max}, Pr^{min}	90-30 (psi)	S^{gas}	0.06014 ($/m^3)
S^{fit}, S^{cur}	0.14, 3.5 ($/km)	$P_i^{Min,gt}, P_i^{Max,gt}$	1000-2000 (kW)
$batt^{cap}$	300-1000 (kWh)	$p2g^{cap}$	200 (kg)
$\mathbb{C}_{ch}^{p2g}, \mathbb{C}_{dch}^{p2g}$	1/40 (kW/kg)	$P_{p2g}^{max}, P_{ESS}^{max}$	1210,600 (kW)
$\eta_{p2g}^{ch}, \eta_{p2g}^{dch}$	0.85	η_{ch}, η_{dch}	0.9
$\mathbb{F}_{i,t}^{flex,MAX}, \mathbb{F}_{i,t}^{flex,MIN}$	130%,70%	β_{comp},η_{comp}	4.7,0.85%
α, b, c	2.148, 2.212, 0.1085	$P_i^{gt,ramp}, P_i^{grid,ramp}$	200,250 (kW)
$\lambda, Z, TEMP, R$	0, 33, 288 (K), 8.314 J/(mol·K)	Δh, cos (θ)	0,0.866 (lag)

Also, the power distribution grid parameters, NGs' ESS specifications, gas turbines' data, and the natural gas grid parameters can be found in [21]. The power grid will supply the remaining demand, which is not matched in the P2P market. As stated before, the scheduling stage, Equations (1)-(43), is performed one day earlier than the executed day. The studied grid's architecture is presented in Fig. 4. The studied microgrid has fifteen NGs, fourteen gas turbines, four P2G units, and one gas compressor located at the beginning of the natural gas network. Also, in the illustrated studied microgrid architecture, LDs refer to NGs. Fig. 5 represents the time of use of the electricity tariff. The predicted electricity and natural gas demands are borrowed from [4, 77].

B. Computational performance

The presented optimization problem is implemented in the Generalized Algebraic Modeling System (GAMS) environment on a computer with a Core i5 system, a 2.50 GHz CPU, and 12 GB of RAM. Due to the nature of the presented optimization problem, which is nonlinear and nonconvex, we solved the presented problem with the global optimizer ANTIGONE solver [78]. The complexity of such problems requires a sophisticated approach, as traditional solvers often fall short of providing feasible and optimal solutions. ANTIGONE's robust framework addresses these challenges by employing advanced algorithms that can efficiently navigate the intricate landscape of nonlinearity and nonconvexity [78]. This solver uses techniques such as branch-and-bound, cutting planes, and outer approximation, which are essential for finding global optima in highly complex optimization scenarios. ANTIGONE uses the CPLEX for solving relaxations, the CONOPT for Finding feasible points, and the LAPACK for Addressing linear systems [78].

TABLE 4 SOLVERS PERFORMANCE.

Modeling	ANTIGONE	DICOPT
Solving Time (min)	15	13
Number of iteration	-	4
Solution gap (%)	17.27%	21.98%

$Gap = 100.\left(\frac{UpperBound - LowerBound}{|LowerBound|}\right)$

To validate the results of the ANTIGONE, we used the DICOPT solver, which decomposes the MINLP problem into sub-problems (NLP) and master problems (MIP). The proposed optimization problem has 99849 variables and 74544 constraints, with 172424 Jacobian elements, of which 26088 are nonlinear.

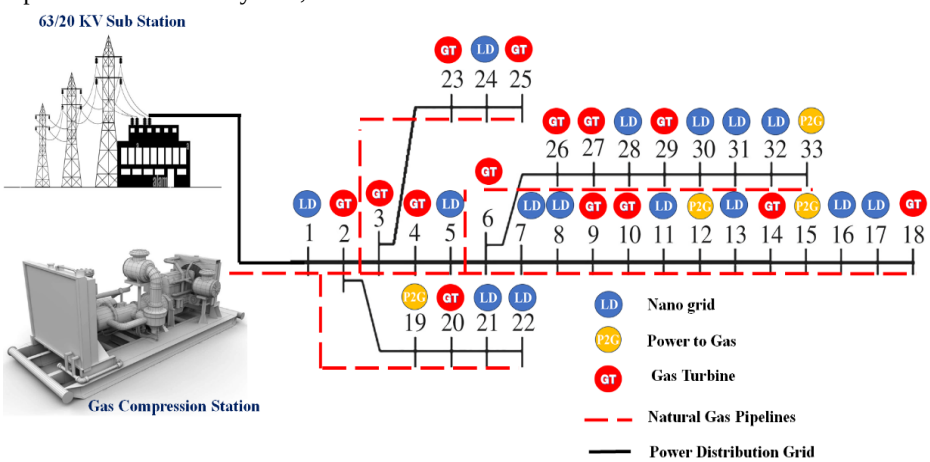


Fig. 4. The studied network architecture.

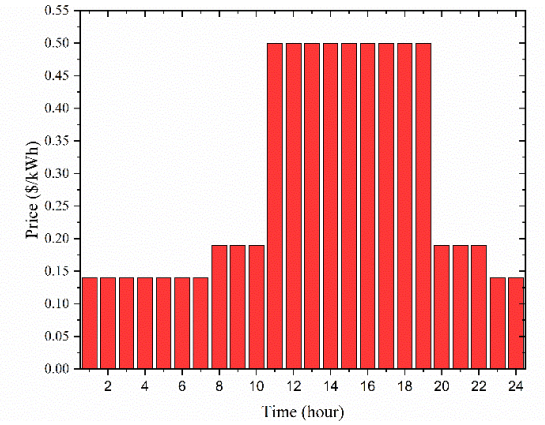


Fig. 5. The electricity tariff.

To assess the performance of the proposed method, we divide the simulations into two sections. Initially, we evaluate the simulation for a single trading period. Subsequently, we extend the simulation to 24 trading periods. Before illustrating the results of the proposed case study, we present a concise description of the method used as a benchmark framework. The proposed method is compared with one common mechanism in the P2P energy trading market, performed in two stages. The technique used as a benchmark framework is the CDA mechanism, comprehensively described in [54], and its implementation procedure is described in Appendix (A.1). Considering that the presented optimization model is based on the scenario-based stochastic optimization problem, a description related to creating scenarios and reducing scenarios is given in Appendix (A.2).

It is worth noting that the benchmark method does not consider the electric distance between purchasers and sellers in the matching process. As a result, the cheapest seller will be sorted first in purchasers' priority lists, while the highest buyer will be sorted first among sellers' preference lists. In the P2P energy trading model based on the CDA framework, through the optimization problem, stage one, the energy schedules of customers are determined. The energy schedules of customers contained the NGs' energy demand pattern and the generated electricity schedules of gas-fired generators. In the following, these schedules are returned to subscribers, and through the CDA method, subscribers trade energy and reach the P2P energy trading agreements.

C. case study (one-period optimization)

In the first case study, we compare the proposed framework with the CDA method for the integrated operation of electricity and natural gas grids at 11 AM. The architecture of the proposed network and the placement of the customers in the low-voltage network are presented in Fig. 4. It is worth noting that both methods use the same input data, which is presented in the previous subsection. In this case, we run the proposed optimization problem, Equations (1)-(43), for one period. The procedure for implementing the CDA framework, the benchmark method, for the integrated operation of gas and power grids is thoroughly described in [4, 54] and Appendix (A1).

Figs. 6 and 7 show traded energy flows during 11 AM between customers without the P2P market and with the CDA-based P2P market, respectively. Without the P2P market, customers trade energy with the power grid. The power grid purchases and sells energy from and to the customers based on the energy retail price, which is not competitive compared to the P2P market price.

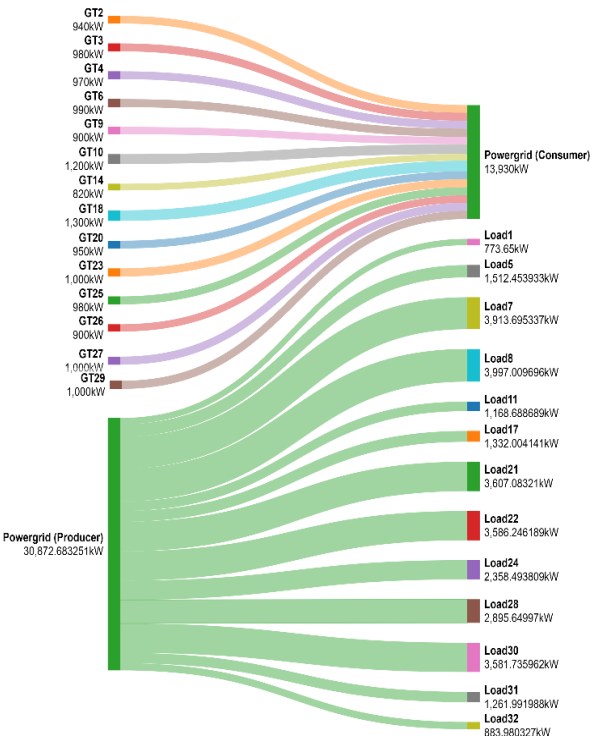


Fig. 6. Energy transactions between customers and the power grid without the P2P market.

As stated, we compare the proposed framework with the previous P2P market-based model as a benchmark method, performed in separate stages. The energy traded flow between customers in the benchmark method is shown in Fig. 7. The power grid balances the energy shortage via retail price (the TOU tariff and the FIT rate). Without the P2P market (Fig. 6) and the CDA-based P2P energy market (Fig. 7), P2Gs do not participate in the energy trading process. Without the P2P market, due to P2G units' conversion efficiency on both sides (charge and discharge), it is not cost-effective for P2Gs to be charged through the power grid via the TOU tariff and discharged to the grid via the FIT rate. Additionally, considering that the previous P2P market model (CDA-based) is executed in two distinct stages (scheduling and trading), a MINLP optimization problem based on the energy retail price is solved during the scheduling stage, similar to the case without the P2P market. Customers engage in energy trading in the subsequent trading stage, which is determined in the

scheduling stage. In this context, similar to the scenario without a P2P market, P2Gs do not participate in energy trading.

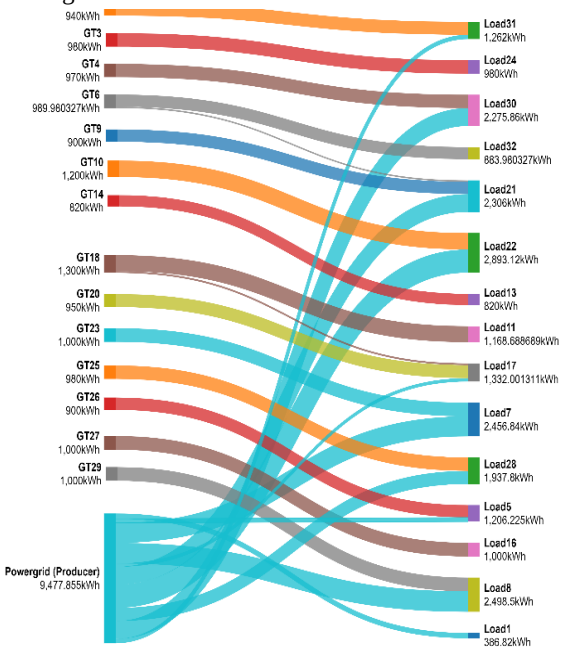


Fig. 7. The flow of the traded energy (the benchmark method).

Figs. 8 and 9 illustrate the proposed method's traded energy flow between customers (NGs, gas-fired units, P2Gs, and the power grid) for different scenarios. There are two significant differences between the proposed method (Figs. 8 and 9) and the previous framework (Fig. 7). First, NGs trade energy with the closest producers in the presented method due to employing the electrical distance model based on the TID framework. Implementing the TID model leads to a situation in which far-off trades impose higher customer costs (reducing gas turbines and P2Gs' revenue and increasing payment costs of NGs). Second, since the proposed method is executed in one stage, the energy consumption and production schedules are determined based on the market competitive price, which leads to the participation of P2Gs in the P2P market.

The right-hand sides of Figs. 8 and 9 represent the energy trading flow in scenarios two and four consecutively. Also, the left-hand side of Figs 8 and 9 illustrate the transacted energy flow in scenarios one and three, respectively. Due to the higher predicted power demand shown in Fig. a3, the volume of traded energy in scenario four is the highest, followed by scenarios two, three, and one. It is worth noting that scenario one has the highest predicted demand for natural gas (Fig. (a4)), which is one reason for reducing traded energy in scenario one. In other words, the DSO limits gas turbines' generated power due to high natural gas demand at period 11 of scenario one to keep node gas pressure in the desired range.

P2Gs are charged during off-peak periods (1-7) through different markets, and due to higher energy prices, they are willing to trade the stored energy during peak hours (11-19). P2Gs supply NGs' power demand through correlation with gas turbines. In other words, when gas turbines can not meet the energy demand of NGs, NGs trade energy with P2Gs. In this regard, P2Gs trade energy with NGs during hour 11 since gas turbines' generated power is reduced due to high natural gas demand in scenario one (Fig (a4))).

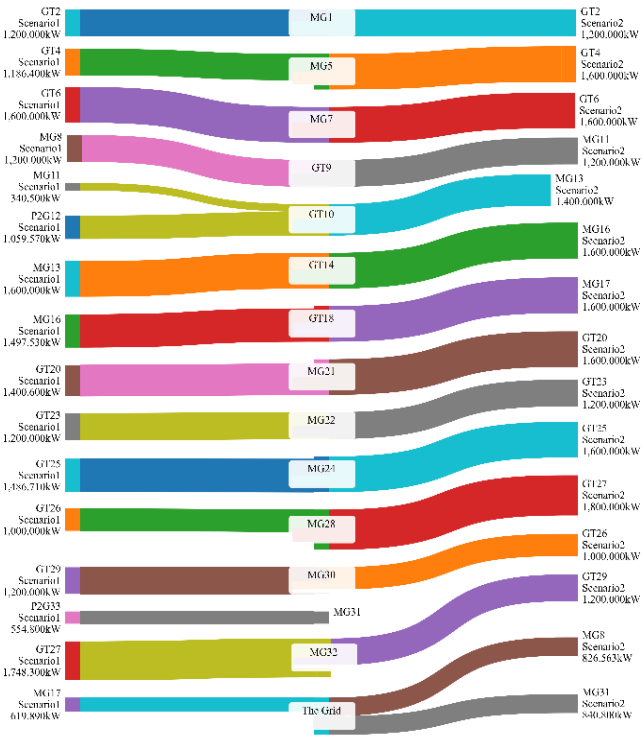


Fig. 8. The flow of the traded energy in scenarios one and two (the proposed method).

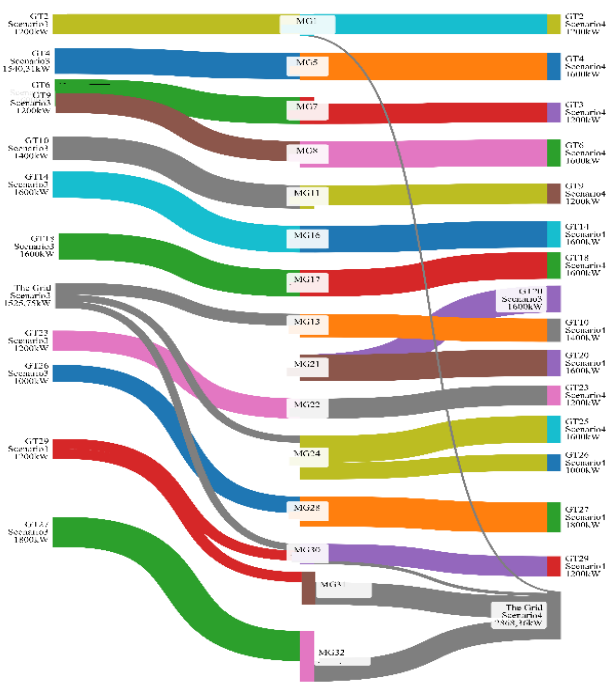


Fig. 9. The flow of the traded energy in scenarios three and four (the proposed method).

Also, due to the high electricity demand in scenario four, the traded energy between the power grid and NGs in scenario four is about 13% of the energy demand of NGs at hour 11, which is the highest among scenarios. Also, it is worth noting that the volume of traded energy in the proposed method is increased by about 40.21% compared to the benchmark method.

Power losses occur during electricity transmission from one bus to another, particularly in P2P energy trading, where electricity is transferred from producers to NGs. As electricity flows through power lines and transformers, some energy is lost due to resistance in the wires and transformers. This phenomenon can result in reduced yields for participants in P2P energy trading. In this context, we evaluate the impact of incorporating the TID model into the proposed method by comparing it with the benchmark framework. Each line's power loss is calculated by dividing energy loss by the line flow. The active power loss in the proposed method and benchmark framework is 26.73% and 47.97358%, consecutively. The power loss reduction in the presented method is mainly due to employing the TID framework in the P2P energy trading process.

The operational cost of the entire network is calculated as the total payment costs of NGs, including the traded energy with gas turbines, P2G units, and power utility, minus the total revenue generated by gas turbines and P2G units from selling power to the grid and NGs. The operating cost of the entire network (hour 11) in the proposed method and benchmark framework is 750.86 ($) and 4738.5 ($), respectively.

D. 24-hour optimization

This section evaluates the performance of the presented method for the entire period of the next day. First, the energy purchased and supplied by the studied network's customers (NGs, gas turbines, and P2Gs) is analyzed. Figs. 10 to 13 illustrate the electricity demand of NGs provided by the power grid and the local market's producers for scenarios one to four consecutively. In the following Figs (10-13), the orange, green, and purple curves are supplied electricity by the power grid and purchased energy from gas-fired generators and P2G units, respectively. As energy traded between P2Gs and NGs clearly shows, P2Gs trade energy mainly after hour 12 due to high natural gas demand (Fig. (a4)). In other words, P2Gs complement gas-fired generators in supplying NGs' energy demand during peak hours.

The upstream grid-supplied NGs power demand during the off-peak period (hours 1-7). With the increase of the energy tariff starting from the mid-peak period (hours 8 to 11), the electricity imported from the power grid decreases. Due to the high energy tariffs, the proportion of energy imported from the power grid during peak periods is minimal, accounting for 20.11%, 11%, 20%, and 20% in scenarios one through four, respectively. After peak periods (hour 20), the amount of imported electricity from the power grid gradually increases.

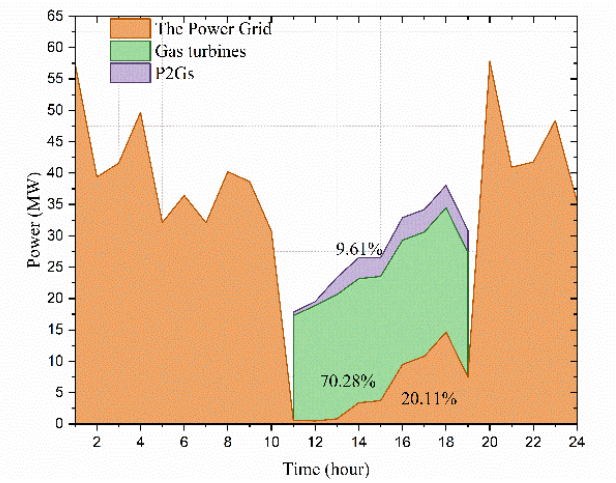


Fig. 10. NGs traded energy in scenario one.

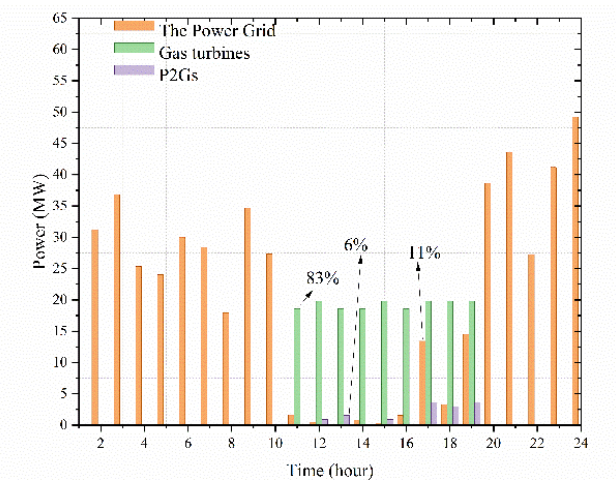


Fig. 11. NGs traded energy in scenario two.

The operational cost of gas-fired generators depends on the gas compressor's electricity demand and gas turbines' natural gas demand. Hence, since the power grid supplies the gas compressor through the electricity tariff, selling power to the grid is cost-effective for gas-fired generators only during off-peak periods. Also, since the P2P market price is cleared between a range in which the TOU and the FIT rates are its upper and lower bounds, respectively (constraint (12)), there is no significant difference between the TOU rate and the P2P market price during off-peak hours. On the other hand, since P2Gs can store energy, they purchase energy from gas-fired generators during off-peak periods and trade the stored energy with NGs during peak hours. Briefly, in off-peak hours, gas turbines trade energy with the power grid and P2Gs, and during peak hours, NGs trade energy with P2Gs, gas turbines, and the power grid. Also, during peak periods, about (70% to 80%), (10% to 20%), and (5% to 10%) of the NGs' power demand is supplied by gas turbines, the power grid, and P2Gs, consecutively.

Due to high electricity prices in mid-peak and peak periods, gas-fired generators trade energy in the P2P market during

these hours. P2Gs are charged during off-peak and mid-peak periods and sell their stored energy to NGs during peak periods. The power grid balances the shortage of energy production. Also, the total operating cost of both networks for the proposed method and the benchmark framework is 115343.2 ($) and 218779.44 ($), respectively. The total operation cost of the entire network in the proposed method is reduced by 47% compared to the benchmark method. The participation of the P2Gs and the increasing generated power of gas-fired generators are the reasons for the significant reduction of the operation cost compared to the previous method.

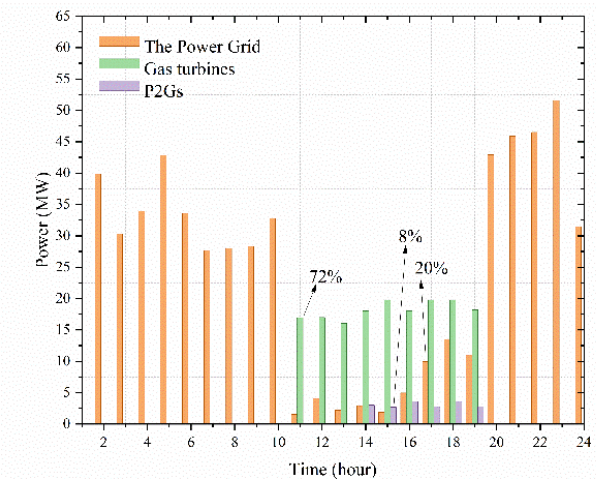


Fig. 12. NGs traded energy in scenario three.

The charging/discharging cycles and the stored hydrogen of the total P2G units are illustrated in Figs. 14-15, consecutively. During periods 1 to 10, P2Gs are charged by the gas turbines through the P2P market (upper side of Fig. 14). By 11 AM, hydrogen containers are charged to approximately 80% of their capacity. With the initiation of the peak periods, the P2Gs trade energy with NGs through the P2P market. The purchased and sold energy costs in the P2P market are 3025.8 ($) and 6916.1 ($), respectively. In this regard, the total P2G revenue from participation in the P2P market is 3891.32 ($/day). The charging energy of P2Gs' is highest in scenario one since during peak hours (periods 11 to 19), the predicted electricity demand of scenario one is highest. In other words, since NGs are only customers for P2G units, their higher energy demand causes P2Gs to be willing to increase their stored energy to trade with NGs during peak hours.

Figs. 16 to 19 represent gas turbines' traded energy in scenarios one to four, respectively. Also, gas compressor power demand is shown in Fig. 20. Gas turbines trade energy with the power grid and P2Gs during off-peak periods. Due to the low electricity tariff during these periods (off-peak), NGs' are not interested in trading energy in the P2P market. Since the gas compressor purchases its required energy from the power grid through the energy retail price, the volume of gas turbines traded energy with the power grid considerably decreases after off-peak periods.

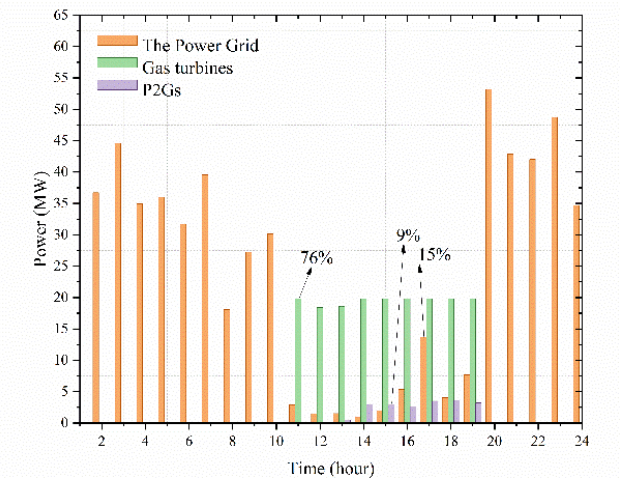


Fig. 13. NGs traded energy in scenario four.

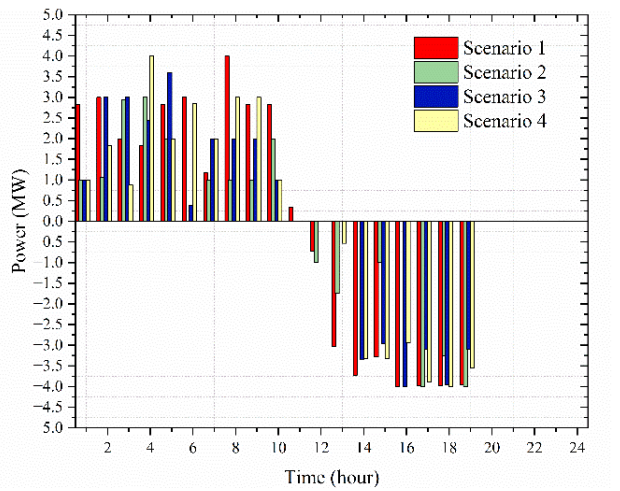


Fig. 14. P2Gs charge and discharge.

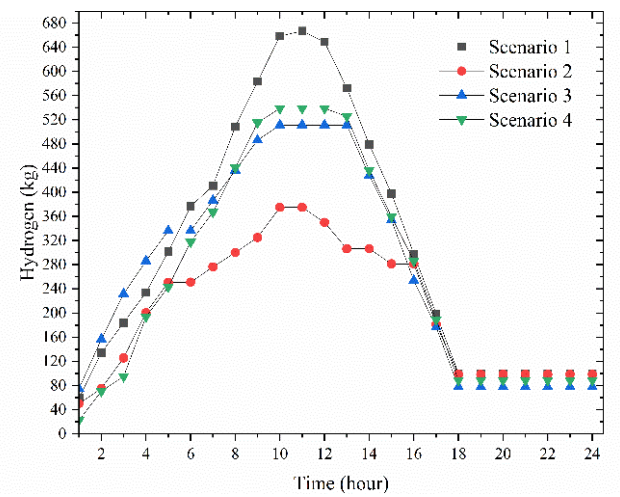


Fig. 15. The stored hydrogen in the containers.

Gas turbines' energy trading with P2Gs continues even in mid-peak periods (hours 8-10). Since P2Gs will sell the stored energy during peak periods, purchasing electricity during mid-

peak periods is cost-effective. Gas-fired generators trade energy with NGs during peak periods. In other words, selling energy via the P2P market at competitive prices makes energy production for gas turbines during peak periods affordable. The cost of supplying natural gas and gas compressor electricity demand are 12993.4 and 4981.3 ($), respectively.

The income of the total gas turbines from selling energy to the power grid (through the FIT rate), P2Gs (P2P market), and NGs (P2P market) are 26829.3, 2733.582, and 42526.41 ($), consecutively. The total revenue of gas-fired generators in the proposed framework and the benchmark method are 59075.71 and 55200.45 ($). Hence, the total revenue of gas-fired generators in the proposed framework is increased by about 7%.

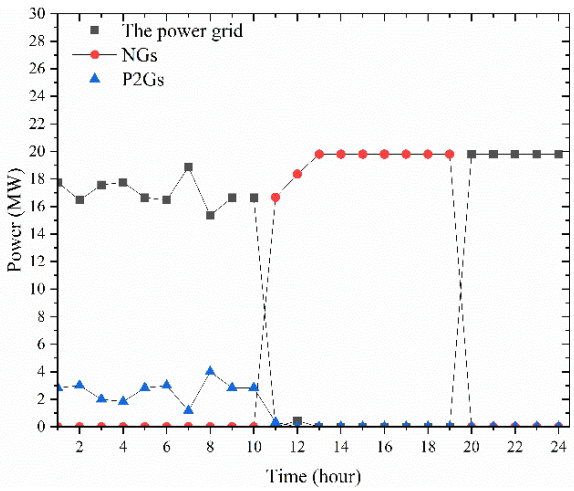


Fig. 16. Gas-fired generators traded energy in scenario one.

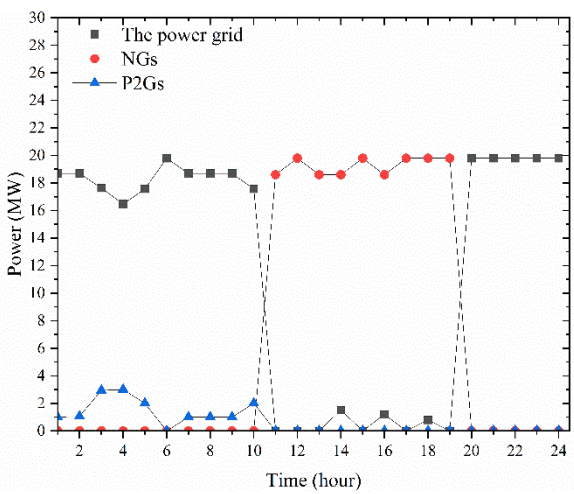


Fig. 17. Gas-fired generators traded energy in scenario two.

Also, as it is clear from Fig. 20, the power demand of the gas compressor is dependent on predicted natural gas demand for different scenarios (Fig. (a4)). Figs. 21 and 22 illustrate the total charging and discharging cycles and the state of charge of entire ESSs for different scenarios. Each NG is equipped with an ESS, which is charged during off-peak periods or hours when NGs trade energy with gas turbines via the P2P market. In order to maximize the usage of gas-fired generators during peak periods, ESSs are charged. Notably, ESS's charging power is supplied by NGs purchased energy. In other words, NGs store a part of the traded energy with the power grid during off-peak periods in ESSs and use it during high energy price periods. Also, Fig. 23 represents the average node gas pressure for different natural gas nodes. As it is clear, during the synergy between natural gas and electricity grids, the presented method guarantees the performance of the natural gas network. Gas pressure reduction alongside nodes (1 to 18) is higher in scenario four, followed by scenarios one, two, and three. The difference between scenarios is caused by differences in predicted natural gas demand for different scenarios, shown in Fig. (a4).

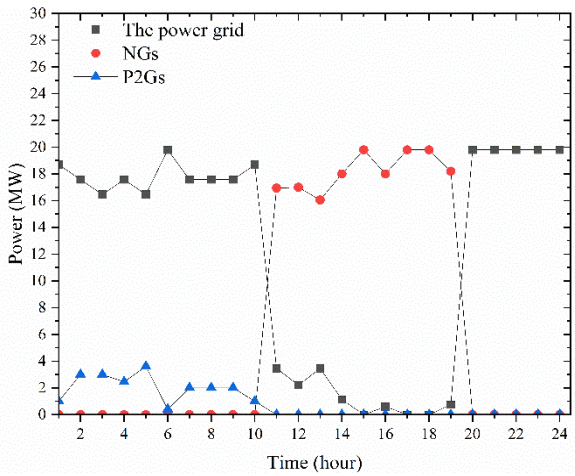


Fig. 18. Gas-fired generators traded energy in scenario three.

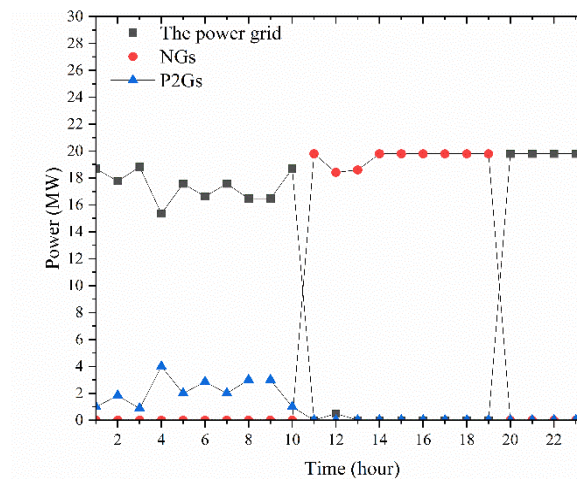


Fig. 19. Gas-fired generators traded energy in scenario four.

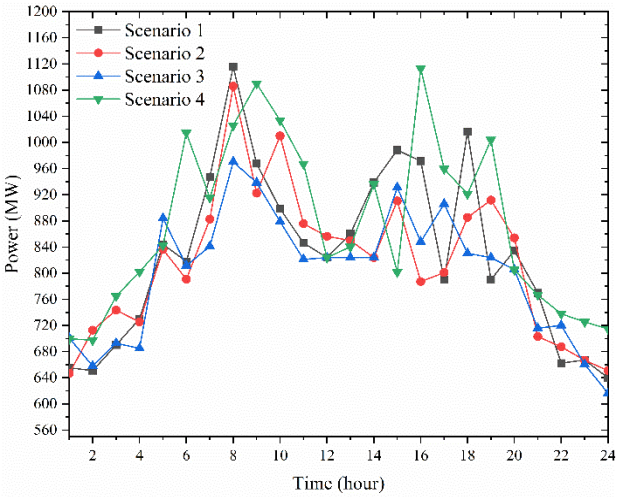


Fig. 20. Gas compressor power demand.

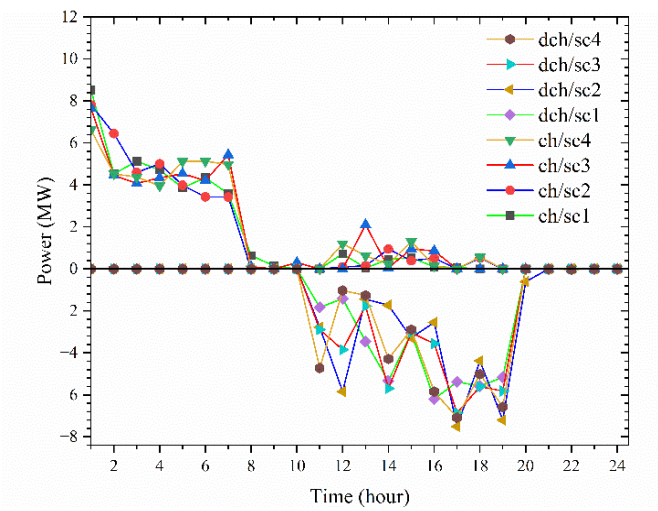


Fig. 21. Total ESSs charging and discharging cycles.

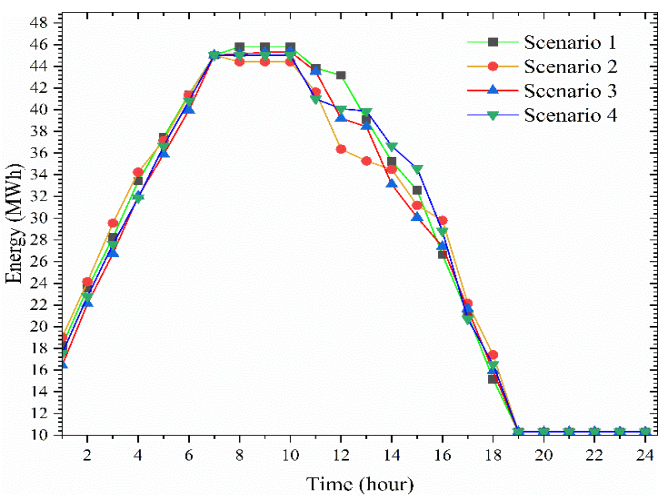


Fig. 22. The state of charge of entire ESSs.

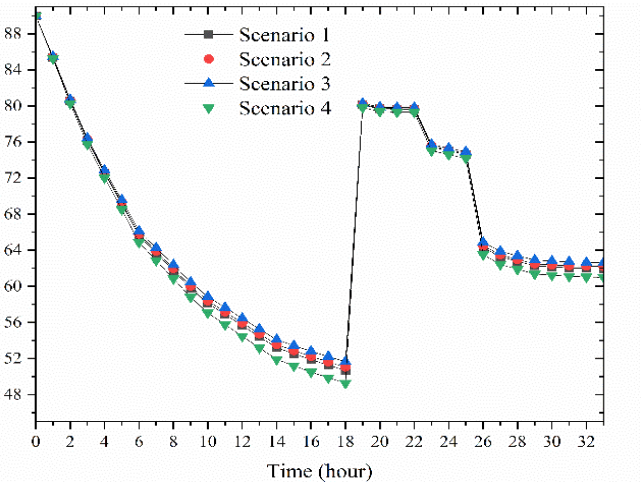


Fig. 23. The average node gas pressure.

V. Conclusion

Due to the importance of coupled operation of the natural gas and electricity grids, this paper proposed a novel stochastic P2P market-based method to integrate the operation of electricity and natural gas networks considering P2G storages, electrical distance, ESSs, DR, and both grid constraints. The presented method was compared with the previous framework as a benchmark method.

In the first step, 1000 random scenarios are generated based on normal PDF. In the following, generated scenarios are reduced by the backward method to four scenarios representing their original generation. Finally, the proposed method is solved for 4 reduced scenarios, and its results are analyzed. The case study was initiated by running the optimization problem for one single trading period. The results of the single-period optimization revealed that employing the TID model in the presented method led to electrically closer trades, reduced power losses by about 44%, and the proposed framework increased the volume of the traded energy by about 40%. Also, it was concluded that without the presented P2P market, P2Gs did not participate in the P2P energy trading process. The separation between the scheduling and trading stage in the benchmark method was the reason for P2Gs not participating.

In the following, the case study was performed for 24 hours. The results revealed the optimum performance of the proposed framework. The total operating cost of the entire network was reduced by about 47%, and the total revenue of gas turbines was increased by about 7% compared to the benchmark method. Also, the entire P2G revenue was 3891 ($), which was zero in the benchmark method. The proposed method could be enhanced by considering electric vehicle parking lots, heat networks, and renewable energy resources.

Appendix (A.1)

A coalition of consumers, producers, and the DSO performs CDA-based P2P energy trading. Unlike the proposed method, the CDA-based P2P energy trading framework is implemented in two distinct stages. In the first step, called the scheduling stage, NGs' electricity energy demands, P2Gs' charging-discharging cycles, and gas turbines' energy production for the next day are determined. Scheduling stage results are obtained by solving the presented optimization in section three, supposing that the customers can only trade with the power grid. In stage two (trading stage), these scheduling results are sent back to customers, and they, based on these energy schedules and the CDA framework, trade energy with each other. Stage two is implemented as follows:

Step 1: Once customers receive the results of the scheduling stage, they initiate energy trading for the next 24 hours by sending bids/offers. The structure of customers' bids is shown by Equation (a1).

$$b_t\left(S_{b,t}, \rho_{b,t}, \delta_{b,t}, \tau_{b,t}\right) \quad \text{(a1)}$$

Where purchaser ($S_{b,t}$) that want to buy ($\rho_{b,t}$) energy in price ($\delta_{b,t}$) at time ($\tau_{b,t}$). Similarly, vendor offer is illustrated by Equation (a2).

$$O_t\left(S_{s,t}, \rho_{s,t}, \delta_{s,t}, \tau_{s,t}\right) \quad \text{(a2)}$$

Step 2: After all offers/bids are received by the DSO for the time slot (t), the DSO creates the order book for the present time slot. The order book is an electronic data sheet that is made for each traded period (hear 24 traded period). In the order book, offers/bids are sorted based on price and arrival time. Offers are sorted in ascending order, and bids are sorted in descending order.

Step 3: Once the order book is ready, if the following relation is satisfied, the purchaser (b_t) and seller (O_t) are chosen for energy trade.

$$\delta_{s,t} \le \delta_{b,t} \quad \text{(a3)}$$

Step 4: The amount of matched energy transaction is calculated by Equation (a4). The following formula indicates the Constraint related to the volume of traded energy. In other words, the minimum preferred energy of the purchaser or seller limits the volume of traded energy. Also, Equation (a5) calculates the matched energy price.

$$\rho_{matched} = min\{\rho_{b,t}, \rho_{s,t}\} \quad \text{(a4)}$$

$$\delta_{matched} = \frac{\delta_{b,t} + \delta_{s,t}}{2} \quad \text{(a5)}$$

Step 5: fully matched bids and offers are eliminated from the order book. Those bids and offers that are not completely matched are updated by Equations (a6) and (a7).

$$b_t'(S_{b,t}, \rho_{b,t}, \delta_{b,t}', \tau_{b,t}) \qquad if\ \rho_{b,t} - \rho_{s,t} > 0 \quad \text{(a6)}$$

$$o_{s,t}'(S_{s,t}, \rho_{s,t}, \delta_{s,t}', \tau_{s,t}) \qquad if\ \rho_{p,t} - \rho_{s,t} < 0 \quad \text{(a7)}$$

Step 6: Repeat steps 1 to 5 for all bids/offers in traded period (t) and continue to period (t+1) if all offers and bids in period (t) are matched.

Appendix (A.2)

Due to considering the uncertainties related to natural gas and power demands, this paper employs the scenario-based stochastic optimization problem. In the first step, 1000 random scenarios (initial samples) are created to represent variations in electricity and natural gas demand. Due to the nonlinear nature of the proposed optimization problem, solving the optimization problem for all created scenarios is time-consuming and impossible. In this regard, the backward reduction method is employed to reduce the number of initial scenarios to four.

The normal distribution function (PDF) is employed to deal with the uncertainty of natural gas and electricity demand, as shown in Equation (a8) [79]. Natural gas and power demand of the studied network is described through mean value (μ) and standard deviation (σ). The σ value for creating natural gas and electricity scenarios is equal to 20%.

$$f(\rho^{g,e}) = \frac{1}{\sqrt{2\pi} \times \sigma^{g,e}} e^{\left(\frac{\rho - \mu^{g,e}}{2\sigma^{g,e^2}}\right)} \quad \text{(a8)}$$

The 1000 generated scenarios for natural gas and electricity demands based on normal PDF are illustrated in Figs. (a1) and (a2), respectivelly. Original scenarios are reduced by the backward reduction method, which is comprehensively described in [80]. Through the backward method, 1000 initial scenarios are reduced to four, of which their occurrence probabilities are 0.37, 0.25, 0.18, and 0.2, respectively.

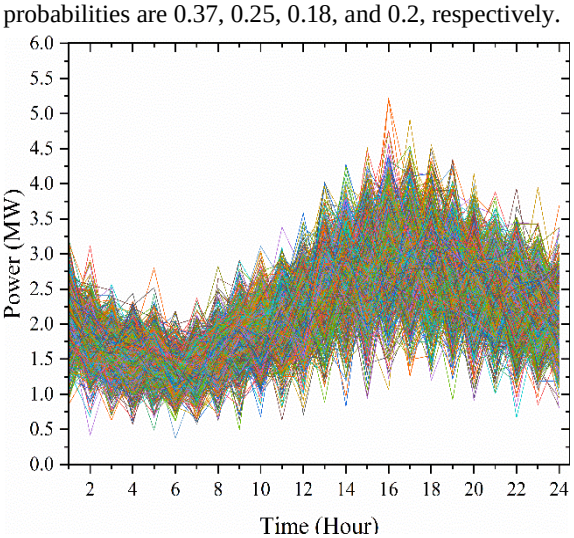


Fig. (a1). Original scenario for electricity demand.

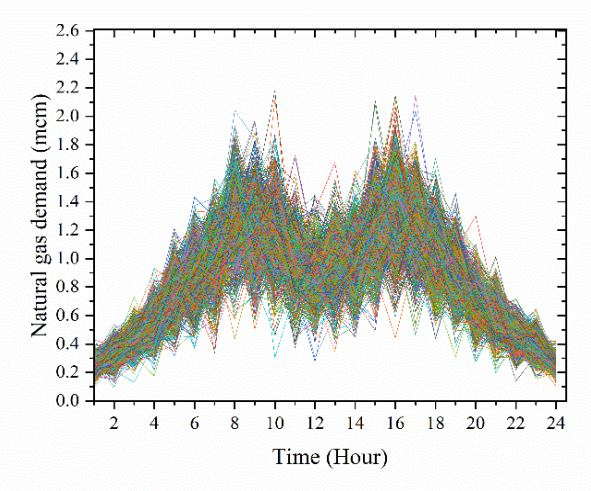


Fig. (a2). Original scenarios for natural gas demand.

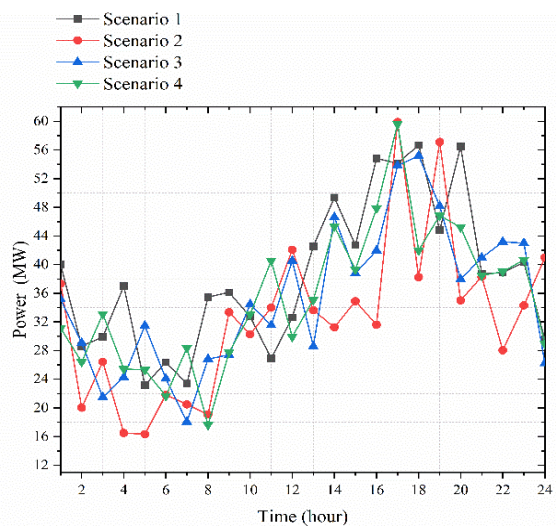


Fig. (a3). Reduced scenarios for natural gas demand.

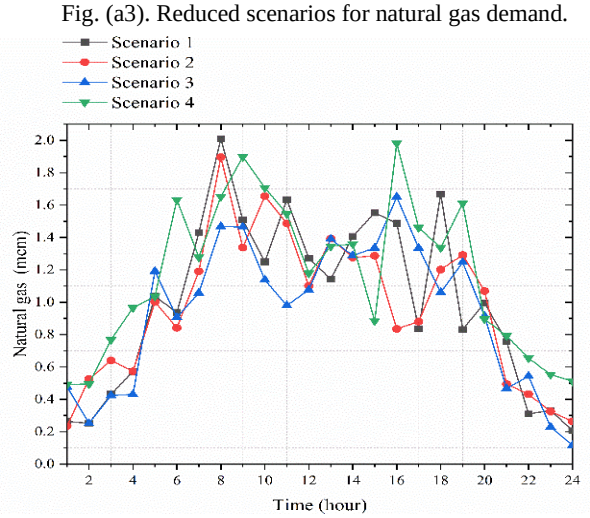


Fig. (a4). Reduced scenarios for natural gas demand.

REFERENCES

[1] R. Zhang, S. Bu, and G. Li, "Multi-market P2P trading of cooling–heating-power-hydrogen integrated energy systems: An equilibrium-heuristic online prediction optimization approach," *Applied Energy*, vol. 367, p. 123352, 2024.

[2] J. Chen, B. Sun, Y. Li, R. Jing, Y. Zeng, and M. Li, "Credible capacity calculation method of distributed generation based on equal power supply reliability criterion," *Renewable Energy*, vol. 201, pp. 534-547, 2022.

[3] Y. Shang, L. Zhu, F. Qian, and Y. Xie, "Role of green finance in renewable energy development in the tourism sector," *Renewable Energy*, vol. 206, pp. 890-896, 2023.

[4] M. Feili and M. T. Ameli, "Integrated operation of gas and power system through the P2P market mechanism," *IET Smart Grid*, vol. 6, no. 4, pp. 359-379, 2023.

[5] A. Masoudi, M. Simab, H. Akbarj, S. A. Saeed, and T. Daemi, "Maximizing the Electric Vehicles' Owners Profit Considering Optimal Charging and Discharging Management in the Distribution Networks Using Dynamic Programming," *International Journal of Industrial Electronics Control and Optimization*, vol. 5, no. 2, pp. 109-121, 2022.

[6] M. F. Akorede, H. Hizam, and E. Pouresmaeil, "Distributed energy resources and benefits to the environment," *Renewable and sustainable energy reviews*, vol. 14, no. 2, pp. 724-734, 2010.

[7] T. Cai, M. Dong, K. Chen, and T. Gong, "Methods of participating power spot market bidding and settlement for renewable energy systems," *Energy Reports*, vol. 8, pp. 7764-7772, 2022.

[8] M. Shafiee, A.-A. Zamani, and M. Sajadinia, "Using improved DDAO algorithm to solve economic emission load dispatch problem in the presence of wind farms," *International Journal of Industrial Electronics Control and Optimization*, vol. 6, no. 3, pp. 161-169, 2023.

[9] C. Wang, J. Wu, J. Ekanayake, and N. Jenkins, *Smart electricity distribution networks*. CRC Press, 2017.

[10] M. Feili, M. T. Ameli, and M. Shafiekhah, "Coupled Energy Systems Operation Through MINLP Framework Considering Systems Constraints and Demand Response," in *2023 13th Smart Grid Conference (SGC)*, 2023: IEEE, pp. 1-8.

[11] Z. Zhang, F. M. Altalbawy, M. Al-Bahrani, and Y. Riadi, "Regret-based multi-objective optimization of carbon capture facility in CHP-based microgrid with carbon dioxide cycling," *Journal of Cleaner Production*, vol. 384, p. 135632, 2023.

[12] Y. Duan, Y. Zhao, and J. Hu, "An initialization-free distributed algorithm for dynamic economic dispatch problems in microgrid: Modeling, optimization and analysis," *Sustainable Energy, Grids and Networks*, p. 101004, 2023.

[13] A. Taghieh, A. Mohammadzadeh, C. Zhang, N. Kausar, and O. Castillo, "A type-3 fuzzy control for current sharing and voltage balancing in microgrids," *Applied Soft Computing*, vol. 129, p. 109636, 2022.

[14] Z. Shi, H. Liang, S. Huang, and V. Dinavahi, "Distributionally robust chance-constrained energy management for islanded microgrids," *IEEE Transactions on Smart Grid*, vol. 10, no. 2, pp. 2234-2244, 2018.

[15] M. Ghiasi, Z. Wang, M. Mehrandezh, S. Jalilian, and N. Ghadimi, "Evolution of smart grids towards the Internet of energy: Concept and essential components for deep decarbonisation," *IET Smart Grid*, 2022.

[16] Z. Shuai *et al.*, "Microgrid stability: Classification and a

review," *Renewable and Sustainable Energy Reviews,* vol. 58, pp. 167-179, 2016.
[17] Y. Zahraoui, T. Korõtko, A. Rosin, T. E. K. Zidane, H. Agabus, and S. Mekhilef, "A Competitive Framework for The Participation Of Multi-Microgrids in The Community Energy Trading Market: A Case Study," *IEEE Access,* 2024.
[18] M. Vosoogh, M. Rashidinejad, A. Abdollahi, and M. Ghaseminezhad, "Efficient networked microgrid management considering plug-in electric vehicles and storage units," *International Journal of Industrial Electronics Control and Optimization,* vol. 4, no. 2, pp. 245-255, 2021.
[19] H. Mei, Y. Li, C. Suo, Y. Ma, and J. Lv, "Analyzing the impact of climate change on energy-economy-carbon nexus system in China," *Applied Energy,* vol. 262, p. 114568, 2020.
[20] D. Forfia, M. Knight, and R. Melton, "The view from the top of the mountain: Building a community of practice with the gridwise transactive energy framework," *IEEE Power and Energy Magazine,* vol. 14, no. 3, pp. 25-33, 2016.
[21] M. Feili and M. T. Ameli, "Integrated operation of gas and power system through the P2P market mechanism," *IET Smart Grid,* 2023.
[22] B. Zheng, W. Wei, Y. Chen, Q. Wu, and S. Mei, "A peer-to-peer energy trading market embedded with residential shared energy storage units," *Applied Energy,* vol. 308, p. 118400, 2022.
[23] O. Jogunola *et al.*, "Peer-to-Peer Local Energy Market: Opportunities, Barriers, Security and Implementation Options," *IEEE Access,* 2024.
[24] R. Safipour and M. Oukati Sadegh, "Optimal Planning of energy storage systems using symbiotic organisms search algorithm," *International Journal of Industrial Electronics Control and Optimization,* vol. 1, no. 1, pp. 19-26, 2018.
[25] Y. Meng, J. Qiu, C. Zhang, G. Lei, and J. Zhu, "A Holistic P2P market for active and reactive energy trading in VPPs considering both financial benefits and network constraints," *Applied Energy,* vol. 356, p. 122396, 2024.
[26] J. Hao, T. Huang, Y. Sun, X. Zhan, Y. Zhang, and P. Wu, "Optimal Prosumer Operation with Consideration for Bounded Rationality in Peer-to-Peer Energy Trading Systems," *Energies,* vol. 17, no. 7, p. 1724, 2024.
[27] A. Tiwari, B. K. Jha, and N. M. Pindoriya, "Multi-objective optimization based demand response program with network aware peer-to-peer energy sharing," *International Journal of Electrical Power & Energy Systems,* vol. 157, p. 109887, 2024.
[28] X. Wang *et al.*, "Congestion management under peer-to-peer energy trading scheme among microgrids through cooperative game," *Energy Reports,* vol. 8, pp. 59-66, 2022.
[29] J. L. Crespo-Vazquez, T. AlSkaif, Á. M. González-Rueda, and M. Gibescu, "A community-based energy market design using decentralized decision-making under uncertainty," *IEEE Transactions on Smart Grid,* vol. 12, no. 2, pp. 1782-1793, 2020.
[30] G. Sun, J. Sun, S. Chen, Z. Wei, and H. Zang, "Market-based coordination of regional electric and natural gas systems: A peer-to-peer energy trading model," *CSEE Journal of Power and Energy Systems,* 2022.
[31] Z. Wang, X. Yu, Y. Mu, H. Jia, Q. Jiang, and X. Wang, "Peer-to-Peer energy trading strategy for energy balance service provider (EBSP) considering market elasticity in community microgrid," *Applied Energy,* vol. 303, p. 117596, 2021.
[32] M. H. Ullah and J.-D. Park, "DLMP integrated P2P2G energy trading in distribution-level grid-interactive transactive energy systems," *Applied Energy,* vol. 312, p. 118592, 2022.
[33] L. Ali, S. Muyeen, H. Bizhani, and A. Ghosh, "A multi-objective optimization for planning of networked microgrid using a game theory for peer-to-peer energy trading scheme," *IET Generation, Transmission & Distribution,* vol. 15, no. 24, pp. 3423-3434, 2021.
[34] K. Rowe, G. Mokryani, K. Cooke, F. Campean, and T. Chambers, "Bi-level optimal sizing, siting and operation of utility-scale multi-energy storage system to reduce power losses with peer-to-peer trading in an electricity/heat/gas integrated network," *Journal of Energy Storage,* vol. 83, p. 110738, 2024.
[35] D. Peng, H. Xiao, W. Pei, H. Sun, and S. Ye, "A novel deep learning based peer-to-peer transaction method for prosumers under two-stage market environment," *IET Smart Grid,* 2022.
[36] N. Tarashandeh and A. Karimi, "Peer-to-peer energy trading under distribution network constraints with preserving independent nature of agents," *Applied Energy,* vol. 355, p. 122240, 2024.
[37] W. Tushar *et al.*, "A coalition formation game framework for peer-to-peer energy trading," *Applied Energy,* vol. 261, p. 114436, 2020.
[38] C. Wang, W. Wei, J. Wang, F. Liu, and S. Mei, "Strategic offering and equilibrium in coupled gas and electricity markets," *IEEE Transactions on Power Systems,* vol. 33, no. 1, pp. 290-306, 2017.
[39] M. Niu, C. Gao, G. Muñoz-Delgado, and J. Contreras, "A cross-carrier multilateral trading model for integrated electricity and natural gas systems," *Applied Energy,* vol. 354, p. 122064, 2024.
[40] A. G. Daryan, A. Sheikhi, and A. A. Zadeh, "Peer-to-Peer Energy sharing Among Smart Energy Hubs in an integrated Heat-Electricity Network," *Electric Power Systems Research,* vol. 206, p. 107726, 2022.
[41] S. Ge, J. Li, X. He, and H. Liu, "Joint energy market design for local integrated energy system service procurement considering demand flexibility," *Applied Energy,* vol. 297, p. 117060, 2021.
[42] M. I. Azim, W. Tushar, and T. K. Saha, "Coalition graph game-based P2P energy trading with local voltage management," *IEEE Transactions on Smart Grid,* vol. 12, no. 5, pp. 4389-4402, 2021.
[43] T. Lu, Z. Wang, Q. Ai, and W.-J. Lee, "Interactive model for energy management of clustered microgrids," *IEEE Transactions on Industry Applications,* vol. 53, no. 3, pp. 1739-1750, 2017.
[44] K. Wang *et al.*, "Embedding P2P transaction into demand response exchange: A cooperative demand response management framework for IES," *Applied Energy,* vol. 367, p. 123319, 2024.
[45] A. Basnet and J. Zhong, "Integrating gas energy storage system in a peer-to-peer community energy market for enhanced operation," *International Journal of Electrical Power & Energy Systems,* vol. 118, p. 105789, 2020.
[46] N. Wang, Z. Liu, P. Heijnen, and M. Warnier, "A peer-to-peer market mechanism incorporating multi-energy coupling and cooperative behaviors," *Applied Energy,* vol. 311, p. 118572, 2022.
[47] W. Zhou, Y. Wang, F. Peng, Y. Liu, H. Sun, and Y. Cong, "Distribution network congestion management considering time sequence of peer-to-peer energy trading," *International Journal of Electrical Power & Energy*

Systems, vol. 136, p. 107646, 2022.
[48] Y. Chen, W. Wei, F. Liu, and S. Mei, "A multi-lateral trading model for coupled gas-heat-power energy networks," *Applied energy*, vol. 200, pp. 180-191, 2017.
[49] H. Wang, C. Wang, M. Q. Khan, G. Zhang, and N. Xie, "Risk-averse market clearing for coupled electricity, natural gas and district heating system," *CSEE Journal of Power and Energy Systems*, vol. 5, no. 2, pp. 240-248, 2019.
[50] T. D. Hutty and S. Brown, "P2P trading of heat and power via a continuous double auction," *Applied Energy*, vol. 369, p. 123556, 2024.
[51] H. Zhang, S. Zhang, X. Hu, H. Cheng, Q. Gu, and M. Du, "Parametric optimization-based peer-to-peer energy trading among commercial buildings considering multiple energy conversion," *Applied Energy*, vol. 306, p. 118040, 2022.
[52] T. Gokcek, I. Sengor, B. P. Hayes, and O. Erdinc, "A hierarchical approach for P2P energy trading considering community energy storage and PV-enriched system operator," *IET Generation, Transmission & Distribution*, vol. 16, no. 23, pp. 4738-4749, 2022.
[53] A. Jiang, H. Yuan, and D. Li, "A two-stage optimization approach on the decisions for prosumers and consumers within a community in the Peer-to-peer energy sharing trading," *International Journal of Electrical Power & Energy Systems*, vol. 125, p. 106527, 2021.
[54] Y. Zhou, J. Wu, G. Song, and C. Long, "Framework design and optimal bidding strategy for ancillary service provision from a peer-to-peer energy trading community," *Applied Energy*, vol. 278, p. 115671, 2020.
[55] N. Hashemipour, P. C. del Granado, and J. Aghaei, "Dynamic allocation of peer-to-peer clusters in virtual local electricity markets: A marketplace for EV flexibility," *Energy*, vol. 236, p. 121428, 2021.
[56] Y. Xia, Q. Xu, J. Fang, Y. Huang, L. Shi, and F. Wu, "Surrogate model enabled integrated energy system trading in buildings considering bidding characteristics," *Energy and Buildings*, vol. 306, p. 113939, 2024.
[57] C. S. Lai, M. Yan, X. Li, L. L. Lai, and Y. Xu, "Coordinated Operation of Electricity and Natural Gas Networks with Consideration of Congestion and Demand Response," *Applied Sciences*, vol. 11, no. 11, p. 4987, 2021.
[58] S. Rezaei and A. Ghasemi, "Stochastic scheduling of resilient interconnected energy hubs considering peer-to-peer energy trading and energy storages," *Journal of Energy Storage*, vol. 50, p. 104665, 2022.
[59] M. Khorasany, A. S. Gazafroudi, R. Razzaghi, T. Morstyn, and M. Shafie-khah, "A framework for participation of prosumers in peer-to-peer energy trading and flexibility markets," *Applied Energy*, vol. 314, p. 118907, 2022.
[60] M. Mehdinejad, H. Shayanfar, and B. Mohammadi-Ivatloo, "Peer-to-peer decentralized energy trading framework for retailers and prosumers," *Applied Energy*, vol. 308, p. 118310, 2022.
[61] S. Malik, M. Duffy, S. Thakur, B. Hayes, and J. Breslin, "A priority-based approach for peer-to-peer energy trading using cooperative game theory in local energy community," *International Journal of Electrical Power & Energy Systems*, vol. 137, p. 107865, 2022.
[62] J. Guerrero, B. Sok, A. C. Chapman, and G. Verbič, "Electrical-distance driven peer-to-peer energy trading in a low-voltage network," *Applied Energy*, vol. 287, p. 116598, 2021.
[63] D. Alkano and J. M. Scherpen, "Distributed supply coordination for power-to-gas facilities embedded in energy grids," *IEEE Transactions on Smart Grid*, vol. 9, no. 2, pp. 1012-1022, 2016.
[64] Y. Zhou, J. Wu, C. Long, and W. Ming, "State-of-the-art analysis and perspectives for peer-to-peer energy trading," *Engineering*, vol. 6, no. 7, pp. 739-753, 2020.
[65] V. Shabazbegian, H. Ameli, M. T. Ameli, G. Strbac, and M. Qadrdan, "Co-optimization of resilient gas and electricity networks; a novel possibilistic chance-constrained programming approach," *Applied Energy*, vol. 284, p. 116284, 2021.
[66] T. Baroche, P. Pinson, R. L. G. Latimier, and H. B. Ahmed, "Exogenous cost allocation in peer-to-peer electricity markets," *IEEE Transactions on Power Systems*, vol. 34, no. 4, pp. 2553-2564, 2019.
[67] D. J. Klein and M. Randić, "Resistance distance," *Journal of mathematical chemistry*, vol. 12, no. 1, pp. 81-95, 1993.
[68] D. Huo, C. Gu, K. Ma, W. Wei, Y. Xiang, and S. Le Blond, "Chance-constrained optimization for multienergy hub systems in a smart city," *IEEE Transactions on Industrial Electronics*, vol. 66, no. 2, pp. 1402-1412, 2018.
[69] M. Geidl and G. Andersson, "Optimal power flow of multiple energy carriers," *IEEE Transactions on power systems*, vol. 22, no. 1, pp. 145-155, 2007.
[70] A. Theerthamalai and S. Maheswarapu, "An effective non-iterative "λ-logic based" algorithm for economic dispatch of generators with cubic fuel cost function," *International Journal of Electrical Power & Energy Systems*, vol. 32, no. 5, pp. 539-542, 2010.
[71] F. Fang, Q. H. Wang, and Y. Shi, "A novel optimal operational strategy for the CCHP system based on two operating modes," *IEEE Transactions on power systems*, vol. 27, no. 2, pp. 1032-1041, 2011.
[72] H. Mehrjerdi, "Peer-to-peer home energy management incorporating hydrogen storage system and solar generating units," *Renewable Energy*, vol. 156, pp. 183-192, 2020.
[73] R. Habibifar, H. Ranjbar, M. Shafie-Khah, M. Ehsan, and J. P. Catalão, "Network-constrained optimal scheduling of multi-carrier residential energy systems: a chance-constrained approach," *Ieee Access*, vol. 9, pp. 86369-86381, 2021.
[74] Y. Jiang *et al.*, "Coordinated operation of gas-electricity integrated distribution system with multi-CCHP and distributed renewable energy sources," *Applied energy*, vol. 211, pp. 237-248, 2018.
[75] G. L. Torres, V. H. Quintana, and G. Lambert-torres, "Optimal power flow in rectangular form via an interior point method," in *Proc. of 1996 IEEE North American Power Symposium*, 1996: Citeseer.
[76] V. Shabazbegian, H. Ameli, M. T. Ameli, and G. Strbac, "Stochastic optimization model for coordinated operation of natural gas and electricity networks," *Computers & Chemical Engineering*, vol. 142, p. 107060, 2020.
[77] M. Feili and M. Mameli, "Simultaneous operation of electricity and natural gas systems through the P2P energy trading mechanism," *Journal of Modeling in Engineering*, vol. 21, no. 75, pp. 205-224, 2023.
[78] R. Misener and C. A. Floudas, "ANTIGONE: algorithms for continuous/integer global optimization of nonlinear equations," *Journal of Global Optimization*, vol. 59, no. 2, pp. 503-526, 2014.
[79] F. S. Gazijahani, S. N. Ravadanegh, and J. Salehi, "Stochastic multi-objective model for optimal energy exchange optimization of networked microgrids with presence of renewable generation under risk-based

strategies," *ISA transactions*, vol. 73, pp. 100-111, 2018

[80] Z. Li and C. A. Floudas, "Optimal scenario reduction framework based on distance of uncertainty distribution and output performance: II. Sequential reduction," *Computers & Chemical Engineering*, vol. 84, pp. 599-610, 2016.



Meysam Feili received his B.Sc. and M.Sc degrees in electrical engineering, with a focuse on power systems, in 2013 and 2017, respectively. Now, he is a researcher at the Center of Excellence in Power System Studies at Shahid Beheshti University. His current research interests are power distribution systems operation, integrating renewable energies, the local energy markets, and multi-vector energy systems.



Mohammad Taghi Ameli received his B.Sc. degree in electrical engineering from the Technical College of Osnabrück, Germany, in 1988 and his M.Sc. and Ph.D. degrees from the Technical University of Berlin, Berlin, Germany, in 1992 and 1997, respectively. He is a Professor in the Department of Electrical Engineering and the chair of the Research Institute for Electrical Networks at Shahid Beheshti University. He has been the Editor-in-Chief of the International Journal of Research and Technology in Electrical Industry (IJRTEI) since 2020. His research interests include the operation, planning, and control of power and energy systems, integrating renewable energies into the energy system, and smart grids.